REMEDIATION OF DOMESTIC WASTEWATER BY ELECTRO-OXIDATION OF DISSOLVED ORGANIC SUBSTANCES

KINYUA, ESTHER MBUCI (MSc)

I84/38119/2017

A THESIS SUBMITTED IN PARTIAL FULFILLMENT OF THE REQUIREMENTS FOR THE AWARD OF THE DEGREE OF DOCTOR OF PHILOSOPHY (CHEMISTRY) IN THE SCHOOL OF PURE AND APPLIED SCIENCES OF KENYATTA UNIVERSITY

NOVEMBER, 2025

DECLARATION

This thesis is my original work and that it has not been presented for a degree in any other university or for any other award.

Signature_____ Date_____

Kinyua Esther Mbuci **Reg. No. I84/38119/2017**

Department of chemistry

SUPERVISORS

We confirm that the work reported in this thesis was carried out by the candidate under our supervision and has been submitted with our approval as university supervisors.

Signature _____ Date _____

Dr. Isaac W. Mwangi

Department of Chemistry

Kenyatta University

Signature _____ Date _____

Prof. Ruth N. Wanjau

Department of Chemistry

Kenyatta University

Signature _____ Date _____

Prof. Sauda Swaleh

Department of Chemistry

Kenyatta University

DEDICATION

I dedicate this work to God Almighty, our creator and source of all knowledge, inspiration and wisdom. He has inspired me through this journey and gave me strength to persevere. I also dedicate this work to my husband, Alex Maina, for his encouragement and making sure that I give it all and complete what I started. To our lovely children-Louis, Trevor, Leon and Tiana who have all been affected by this quest in many ways and to my friends for their continuous support throughout the study. A special dedication goes to my loving parents Francis and Agnes Kinyua for nurturing my self-confidence and inculcating in me the virtues of hard work. You taught me that I should never give up. Thank you. My love for every one of you is immeasurable. God bless you.

ACKNOWLEDGMENTS

I would like to express my sincere gratitude and appreciation to Dr. Isaac Mwangi, Professor Ruth Wanjau, Professor Sauda Swaleh and the entire staff of the Department of Chemistry, Kenyatta University for their invaluable insights, guidance and wholehearted support throughout my PhD course. The freedom and flexibility they afforded me made things much easier than they would have been. Their encouragement, observations, suggestions and corrections during my presentations were instrumental in ensuring that I went through with this work to the very end.

Special thanks go to my brothers and sisters for their financial support, love and encouragement. Finally, and most importantly, I wish to thank the Almighty God for giving me life and the energy to complete this endeavor.

TABLE OF CONTENTS

LIST OF FIGURES

LIST OF TABLES

ABBREVIATIONS AND ACRONYMS

ADC	Analogue Digital Converters
AOX	Adsorbable Organic Halides
BDD	Boron Doped Diamond
BOD	Biochemical Oxygen Demand
CDOM	Chromophore Dissolved Organic Matter
CE	Counter Electrode
COD	Chemical Oxygen Demand
CR	Counting Resistor
CV	Cyclic Voltammetry
DIC	Dissolved Inorganic Carbon
DMM	Digital Multimeter
DOM	Dissolved Organic Matter
DSA	Dimensionally Stable Anode
EDX	Energy Dispersive X-ray
FTIR	Fourier Transformation Infrared
ISC	Intersystem Crossing
MO	Metal Oxide
MSB	Most Significant Bit
PAni	Polyaniline
PEM	Proton Exchange Membrane
PPy	Polypyrrole
PS	Polysulphone
PT	Polythiophene
PVA	Polyvinyl alcohol
R	Alkyl group
RE	Reference Electrode
RO	Organic Oxides
ROOH	Organic Peroxides
SAR	Successive Approximation Register
SEM	Scanning Electron Microscopy
SCE	Standard Calomel Electrode
SMFC	Sedimentation Microbial Fuel Cell
SPEEK	Sulphonated Poly Ether Ether Ketone
SS	Suspended Solids
TOC	Total Oxygen Carbon
UV-Vis	Ultraviolet Visible Spectroscopy
VSS	Volatile Suspended Solids
WE	Working Electrode
XRD	X-ray Difraction

ABSTRACT

Water pollution poses a significant threat globally, rendering vital water resources unsuitable for sustaining life. Detecting harmful substances dissolved in water can be done by observing changes in its colour, indicating the presence of pollutants like chemicals, trash, bacteria, and parasites. These contaminants alter water's appearance, affecting its clarity and overall quality. Basic methods to improve water clarity involve coagulation and settling techniques, but these can leave residues that lead to health issues. Efforts to treat wastewater have used strong oxidizing agents to eliminate pollutants, but this approach introduces secondary pollutants in treated water. Hence, there's a need for cost-effective techniques for domestic wastewater treatment. This study explores an electrochemical method to remove dissolved organic substances from water. It involves generating reactive oxidizing species at an electrode to interact with these substances. Two types of anode electrodes were used. A platinum electrode and a dimensionally stable anode (DSA) coated with iron (III) doped titanium dioxide on graphite. The incorporation of iron (III) ions within the structure and the crystal form of the material were both confirmed using SEM-EDX and XRD respectively. The experimental setup featured a two-chamber cell divided by a proton exchange membrane (PEM) made from a conducting polyaniline polymer. The polymeric material was characterized using Fourier Transformation Infrared spectroscopy (FTIR). The analysis confirmed the presence of conjugated bonds that can enable conduction of electricity by the organic material. The PEM was casted onto a fritz grid separating the two compartments of the cell. The setup for the oxidation process was done for the treatment of the domestic wastewater to enable a green chemistry treatment method without generating secondary pollutants. Treatment occurred in the anodic chamber where oxidizing species were generated. The platinum anode reduced oxygen from the air, while the DSA facilitated electron and holes generation through photo-oxidation, effectively degrading organic matter. Excess protons were discharged to the cathode through the casted PEM, separating the two halves of the reactor. The cell successfully purified a green leafy solution at 4.5 g/L concentration within 72 hours. Potential measurements reached a high voltage of about 105 mV within the initial 150 minutes of the oxidation process. Monitoring degradation through potential measurements and kinetics confirmed a gradual reduction in dispersed matter concentration over time. These findings illustrate the potential of this degradation process for remediating domestic wastewater, enabling its reuse at the source.

CHAPTER ONE

INTRODUCTION

1.1 Background of the study

Water pollution is a major concern to the global pollution as it renders the blue gold unsuitable for supporting life. Because water is a universal solvent that easily and uniformly disperse soluble nutrients, it contributes greatly to the quality of life on earth (Brini *et al.,* 2017). Even though this dissolving power of water is very important for life, the presence of dissolved pollutants, and especially organic matter contributes to unpleasant color, taste and odor in water. Dissolved organic matter also contribute to reduction in oxygen concentration when decomposers break them into simple organic or inorganic substances utilizing oxygen, and creating an extra demand for dissolved oxygen, resulting to dead zones (Bhateria & Jain, 2016).

One way to determine if water has harmful substances dissolved in it is by observing changes in its color. Pollution often causes water bodies to display unusual colors like black, grey, or red (Xu *et al.,* 2018). These colors indicate the presence of pollutants such as chemicals, trash, bacteria, and parasites. When organic matter dissolves in water, it fosters an environment where bacteria can thrive and contributes to its coloration. This organic matter includes substances like carbohydrates, lignin, fats, soaps, synthetic detergents, proteins, and their breakdown products, which enter the environment when disposed of (Findlay, 2021). These compounds alter water's appearance, affecting its clarity and indicating its quality. Domestic wastewater is one of the major sources of dissolved organic matter.

Pollution due to domestic wastewater is mainly due to human activities in the households. Such waters are largely discharged from the kitchen wash basin, shower, toilet and laundry which is categorized as black water and grey water**.** Black water comprises of human feaces mixed with urine while grey water is water from the sinks in the kitchen, plus effluent from bathrooms and laundry. The main components of domestic wastewater and pollution to the environment is as presented in table 1.1

Table 1.1: Components of domestic wastewater (Henze & Ledin, 2001)

Components	Effects
Pathogenic bacteria, virus and worms, eggs	Disease causing to humans
Detergents, pesticides, fat and grease, coloring, solvents, phenols, cyanide	They are toxic, interfere with aesthetic and bioaccumulate in the food chain
Nitrogen, phosphorus, ammonium	Cause eutrophication and oxygen depletion to aquatic life
Hg, Pb, Cd, Cr, Cu, Ni	Are toxic and bioaccumulate in the environment
Bases and acids such as hydrogen sulphide	Corrosive and toxic
Hot water	Change living conditions for flora and fauna
Odour	Interfere with aesthetic and cause toxic effect
Radioactive substances	Are toxic and they have accumulation effect

The physical properties of domestic wastewater include a grey color with a musty odor. It has solid content of about 0.1% of which about 30% of these solids are suspended and 70% are dissolved (Samer, 2015). Its chemical properties include presence of dissolved organic and inorganic substances as well as dissolved gases. Among the organics are the carbohydrates, proteins and fats reflecting human diet. The inorganics include the heavy metals, sulphur,

phosphorus and other toxic compounds. Gases commonly dissolved in water are methane, ammonia, hydrogen sulphide and nitrogenous compounds. Some of these gases like hydrogen sulphide, ammonia and methane arising from the degradation bio-material in the wastewater. The concentrated domestic wastewater; representing households with low water consumption (20-30 liters per day per household) and dilute wastewater representing households with high water consumption (200 litres or more per day per household). The analysis of parameters in typical domestic wastewater is shown in table 1.2.

Table 1.2: Parameters of domestic wastewater (Henze & Ledin, 2001)

Parameters	**Content in concentrated wastewater for 5 days**
Biochemical oxygen demand (BOD)	350 mg O_2/l
Chemical oxygen demand (COD)	740 mg O_2/l
Total oxygen carbon (TOC)	250 g C/m^3
Suspended solids (SS)	450 g SS/m^3
Volatile suspended solids (VSS)	320 g VSS/m^3
Alkalinity	37 Eqv/m^3
Conductivity	120 mS/min
Total nitrogen	80 g N/m^3
Total phosphorus	23 g P/m^3
Fats, oil and grease	100 g/m^3

A straightforward way to purify water involves employing coagulation and settling techniques. Common water coagulants include ferric chloride, polyaluminum and aluminum sulfate (alum). Aluminum sulfate (commonly used coagulant), research indicates that its residues in water can lead to human diseases such as Alzheimer's disease, bone issues, and kidney problems (Krupińska, 2020). This occurs because aluminium

sulfate undergoes partial hydrolysis, resulting in the production of $Al(OH)_3$ and H^+ ions, as illustrated in equation 1.1.

$$Al^{3+} + 3H_2O \rightarrow Al(OH)_3 + 3H^+ \quad (1.1)$$

Aluminum hydroxide, considered a weak base, does not ionize completely. Due to the partial hydrolysis of aluminium sulphate, its solution turns acidic due to an excess of H^+ ions, signalling a low concentration remaining Al^{3+} ions in the purified water (Krupińska, 2020). Even though the aluminum concentration is low, extended consumption poses a danger to consumers (Jiao *et al.,* 2015).

Another technique for purifying water is electrocoagulation, using an electric current to break down a sacrificial electrode to remove pollutants from wastewater. However, this treatment process has drawbacks: it generates sludge, dissolves the electrode (adding more pollutants), and necessitates periodic replacement of the electrode (Ebba *et al.,* 2022).

In certain water treatment systems, strong oxidizing agents have been employed to treat wastewater by oxidizing pollutants (Bartolomeu *et al.,* 2018). However, this method involves introduction of additional chemical species, resulting in secondary pollutants in the treated water. A common method which does not introduce secondary pollution applied in the treatment of dissolved organic matter in wastewater is by use of hydrogen peroxide (H_2O_2) for the oxidation process. Hydrogen peroxide treatment is suitable for offensive odourant pollutants in aqueous wastes. The only limitation of hydrogen peroxide is that, it involves procurement of the reagent.

To address these limitations, this study investigated an electrochemical approach for *in-situ* oxidation of dissolved organic substances in domestic wastewater, specifically at the point of use. An electrochemical cell was constructed to produce hydrogen peroxide from the wastewater while simultaneously oxidizing dissolved organic matter, thereby purifying it. This method draws inspiration from Microbial Fuel Cell (MFC), a type of bio-electrochemical system that generates electric current by channeling electrons created during microbial oxidation on the anode to reduce molecules, like oxygen, on the cathode through an external electrical circuit. This conversion process turns chemical energy into usable electrical energy (Vishwanathan, 2021). The MFCs are devices that do not involve combustion; instead, they harness microorganisms as biocatalysts, using organic materials as sustenance for these microorganisms. As the microbes metabolize, they convert chemical energy into usable electrical energy (Prakasham & Kumar, 2019).

The components of the microbial fuel cell are electrodes and a two-chambered compartment separated by a proton exchange membrane (PEM). The anode where microorganisms colonize, is the site of oxidation. Electrons are generated from the organic matter and passed onto the electrode surface. As the two electrodes are connected by an external wire, the generated electrons are conducted through to the cathode. The cathode can be surrounded by water or a dilute solution of potassium chloride or potassium ferricyanide. The positively charged hydrogen ions generated at the anode are passed through the PEM to the cathode, and combine with electrons and oxygen ions on the cathode surface to form water, thus completing the electrical circuit (Roy *et al.,* 2023). MFCs for wastewater treatment is a sustainable technology capable of removing organic pollutants and have low energy requirement, which minimizes chemical usage (Aelterman *et al.,* 2006).

The MFCs have low start-ups because they are not electrochemically active. This necessitates need of use of mediators to aid in transferring electrons from the organic molecules to the electrode. Mediators include substances like thionine, methyl viologen, methyl blue, humic acid, and neutral red, that are generally expensive and toxic (Gemünde *et al.,* 2022). On the other hand, mediator-free microbial fuel cells utilize electrochemically active bacteria to directly transfer electrons to the electrode. These bacteria act as catalysts in oxidation of organic substrate, and are capable of transporting electrons from their respiratory enzymes directly to the electrode. Among these electrochemically active bacteria are species such as *Shewanella putrefaciens, Aeromonas hydrophila,* and others. These microbes possess pili on their external membranes, suggesting that for them to function, they need to be present in the anode chamber, potentially leading to the presence of these bacteria in the treated water (Gemma, 2018).

Several studies have investigated the use of MFC in wastewater treatment. The use of an MFC to remove carbon and nitrogen from wastewater was investigated by (Zhao & Song, 2014). They observed a nitrification rate of 17.9 mg·/L, and a COD removal efficiency of 94.1%. Dairy industry wastewater treatment was carried out by (Mansoorian *et al.,* 2016), using a catalyst-less and mediator-less membrane microbial fuel cell and they observed maximum removal efficiency of COD, BOD, NH_3, NH_4^+, dissolved phosphorus, phosphorus in suspended solids, $SO4^{2-}$, TSS, and VSS at 90.46%, 81.72%, 73.22%, 69.43%, 31.18%, 72.45%, 39.43%,70.17% and 64.6% respectively. Sodium dodecyl sulfate (SDS) and organic matter removal using a constructed MFC was investigated by (Sathe et al., 2020), and the system registered a SDS removal efficiency of more than 96%, and organic matter removal efficiency of more than 71%. An on-site sanitary wastewater treatment system was constructed using an MFC by Das et al. (2020). The system recorded a COD removal efficiency of 87.29% after a retention time of 36 hours, while vegetable oil industrial wastewater was treated using an MFC

by Firdous et al. (2018), and the system registered the highest COD removal efficiency of between 80-90% after 72 hours treatment time. While previous studies consistently demonstrate that MFCs are effective in treating wastewater, they all depend on microorganisms as biocatalysts to initiate the oxidation of organic matter. In contrast, this study modifies the MFC design to operate without microbial involvement. Instead of relying on bacteria to drive electron transfer and degradation processes, this system uses an electrochemically active anode to directly oxidize organic pollutants in the wastewater. This approach eliminates the need for microbial growth, maintenance, and retention within the system, thereby addressing concerns related to microbial contamination of treated water and slow startup times associated with microbial colonization.

The setup is inspired by the working of an MFC that has been utilized by Daniel and colleagues, for electricity generation. Their study involved an MFC that relied on bacterial action to oxidize organic matter, leading to the production of electrons at the anode. Subsequently, these electrons moved to the cathode through an external connection, facilitating the redox process (Daniel *et al.,* 2009). Similarly, this study capitalized on electron generation at the anode, but without the involvement of microbes.

1.2 Statement of the problem

The discharge of untreated domestic wastewater into limited freshwater resources poses a major environmental and public health challenge that requires urgent intervention. Conventional wastewater treatment methods such as coagulation, chlorination, and filtration are often costly and energy-intensive. Moreover, these processes may produce harmful byproducts such as sludge and secondary pollutants, further degrading water quality.

Although biological systems such as microbial fuel cells have shown potential in treating wastewater, they are limited by their dependence on microbial activity, slow start-up times, and instability under varying conditions. Similarly, chemical and electrochemical approaches such as electrocoagulation and advanced oxidation processes, while effective, often generate secondary pollution, require sacrificial electrodes, or rely on externally supplied oxidants like hydrogen peroxide, which increase operational cost and complexity.

Therefore, there is a pressing need for an alternative, sustainable wastewater purification method capable of degrading dissolved organic pollutants in-situ, without microorganisms, sacrificial electrodes, or added reagents. This study aims to develop an eco-friendly electrochemical cell that generates reactive species to oxidize organic contaminants directly in wastewater. The proposed system offers a potential point-of-use solution for wastewater treatment, contributing to water recycling and helping mitigate water scarcity in resource-limited environments.

1.3 Justification of the study

Water pollution, being a major concern globally, has been an area that is being continually researched on due to its effect on general human health. Domestic wastewater is one of the

major sources of water pollution. The main treatment methods that have commonly been used are expensive, toxic and harmful because they are used in proportion to the contaminants. This means that the treated water has limited applications due to the introduction of secondary pollutants from the oxidizing agents. The need to treat wastewater using green methods that do not use chemicals that introduce secondary pollution cannot be overemphasized. This is with an aim of averting water pollution and increasing the reusability of domestic wastewater, hence coping with water shortage. The results of this study are of importance to water treatment plants to improve on water treatment methods. The study can also be useful to water resource managers to create better policies on the reusability of wastewater.

1.4 Hypothesis

There is no significant degradation of dissolved organic matter in aqueous media using an electro-oxidation process in a photoactive electrochemical cell incorporating an aniline-based conducting polymer membrane.

1.5 Objective

1.5.1General Objectives

The general objective of the study is to purify domestic wastewater by *in situ* oxidation of dissolved organic substances using an assembled electrochemical cell.

1.5.2 Specific objectives

i. To prepare and characterize an inert conducting polymer synthesized from aniline for use as a proton exchange membrane in the cell
ii. To prepare and characterize a photoactive material for coating on a dimensionally stable anode (DSA) of the cell

iii. To characterize the coated dimensionally stable anode electrode

iv. To determine the degradation kinetics of dispersed organic species in model wastewater solutions using the assembled electrochemical cell with a platinum anode electrode.

v. To determine the degradation kinetics of dispersed organic species in model wastewater solutions using the assembled electrochemical cell dimensionally stable anode.

1.6 Significance of the study

This study offers a significant method of encouraging domestic wastewater recycling at the point of use. It demonstrates that wastewater can be purified at small scale and *in-situ* without adding chemicals that result to harmful by products, contributing towards sustainable development goal 6, 9, 12 and 13.

1.7 Scope and limitations

This study involved the preparation and characterization of a conducting polymer from aniline for use as a proton exchange membrane. It also looked into preparation and characterization of a dimensionally stable anode by coating graphite electrode with iron (III) doped titanium dioxide and fabrication of an electrochemical cell. The assembled cell was used to degrade only the dissolved organic matter in domestic wastewater by monitoring the decontamination process through the variation of potential across the cell and the changes in optical property of the wastewater. The organic dissolved matter from green leafy vegetable of Kale were studied. Organic matter from other vegetable washings water and the subsequent inorganic ions in the matrix were the limitations of the study.

CHAPTER TWO

LITERATURE REVIEW

2.1 Introduction

The growth in population coupled with the high rate of urbanization has resulted in a high demand of water resources while at the same time has affected its quality. From the United Nations world population projections (Leong *et al.,* 2018), the world population will have increased from 7.8 billion in 2020 to 9.74 billion in 2050. This means that there is a projected increase in demand for water. This demand has increased pressure on the existing water resources since high population is not proportional to increase in availability of water resources. The growing population and rising economy has also caused increased discharge of wastewater-leading to heavy pollution of the already scarce resource (Naidoo & Olaniran, 2014). In addition, pollution due to industrial and agricultural activities lowers its supply to the high population and limits its availability for sustainable urban growth. Pollution of this vital commodity does not only reduce the availability of this vital commodity, but also affects the general health of man and the ecosystem. In these circumstances, innovative wastewater techniques need to be developed in order to deal with water shortage issues. Strategies to improve efficiency in water usage, conservation and recycling are key to averting the existing water challenges.

2.2 Analysis of green leafy vegetable solution

The literature extensively discusses the composition of green leafy vegetables, which generally includes water content within a pH range of 2-7, proteins, lipids, starch, and mineral elements such as iron, calcium, phosphorus, and magnesium. When these components are in solution, they dissolve and form a solution representing green leafy vegetables (Mathew, 2000; Natesh *et al.,*2017; Butt & Sultan, 2018; Morris & Mohiuddin,

2020). Such is the composition of domestic wastewater as analyzed previously in literature (Henze & Ledin, 2001). In this study, these dissolved components serve as a model for domestic wastewater that is oxidized by the assembled cell.

2.3 Remediation of domestic wastewater

On-site sanitation measures that include pit latrines as well as septic tanks are largely used in rural and semi-urban areas in Africa. In some cases, such wastes are collected in trucks to wastewater treatment plants for the necessary treatment (de Mello *et al.,* 2018). Several stages which include filtering to remove suspended particles, removal of organic compounds by microbial digestion and then disinfection so as to meet the requirements for discharge are used to purify wastewater. The solids removed from wastewater are then digested through the activated sludge method in what we term as the biological degradation process (de Mello *et al.,* 2018). The biological degradation process of treatment is an economical process in long term operations. However, the process is slow and results into longer periods of storage of wastewater during treatment.

The use of oxidation process of the organic compounds in wastewater using an electrochemical cell has recently attracted attention due to the ease of construction of the treatment plant and its operation. The cell does not require the addition of chemical reagents like in the chemical treatment since the oxidation of the organics takes place at the surface of the electrode (anodes) which are the fixed active sites (Martínez-Huitle & Andrade, 2011). Most water treatment process introduce secondary pollutants which are one of the toxic by-products or require external source of energy. This study envisioned and exploited a treatment process where all the leaching species are consumed in the

electrochemical reactor with no side products and the process requires no external source of energy while ensuring water security.

2.4 The electrochemical wastewater treatment

Electrochemical wastewater treatment is the use of electricity to decontaminate water. This method has been applied using four mechanisms which include coagulation, electrochemical deposition, flotation and oxidation (Özyurt & Camcıoğlu, 2018). Electro-coagulation is a method used to form coagulants mainly from iron and aluminium anodes. The method has been widely studied and applied to purify water to drinking water standards. This electrochemical process electrolytically oxidizes a sacrificial anode to release metal ions into the solution, which interact with the intended pollutants to form coagulants, destabilizing contaminants, and breaking emulsions. This means that metal ions are introduced in the treatment water resulting into introduction of secondary pollution (Zheng *et al.,* 2013).

Deposition is a method that uses the cathode reduction process to remove metals from wastewater by electrically depositing them on the cathode. This technique is used to recover metals from industrial effluents (Tao *et al.,* 2011). Electro-floatation systems are used to generate hydrogen and oxygen gas bubbles from water via electrolysis, and these gases are used to remove suspended solids in wastewater by froth floatation (Matis & Peleka, 2010). This method can only be used to remove sub-micro particles from contaminated water.

The electro-oxidation process refers to enabling electrons being incorporated in the species with high electron affinity of the material of interest. In this case, an oxidation process of organic compounds in polluted water. It can be achieved by applying an electric current or a potential difference between two electrodes (anode and cathode). The system generates strong oxidizing

species when a supporting electrolyte and sufficient energy input are in place. These species interact with pollutants and degrade them. The choice of anode material and the type of electrolyte used determines the generation of oxidizing species during this electrochemical reaction. This oxidation takes place at the anode where organics are completely oxidized to CO_2 and H_2O. The oxidation of organics at the anode can either be direct or indirect depending on the type of anode, and whether a mediator is involved or not (Panizza & Cerisola, 2008). In domestic wastewater, the main pollutants are the organics and microorganisms which are human pathogens dissolved in water. These pollutants can be removed by electrochemical oxidation at the anode of an electrochemical cell (Dbira *et al.,* 2019).

2.4.1 Mechanisms of electrochemical oxidation

An electrochemical oxidation process can be achieved in two different methods. One being the direct oxidation of organics on the surface of the electrode, thus a direct electron transfer or adsorption of oxidant species. The second method is the indirect oxidation by use of mediated oxidant species formed in the bulk solution as shown in scheme 2.1. In this work, direct oxidation method was utilized as the degradation mechanism of the assembled cell.

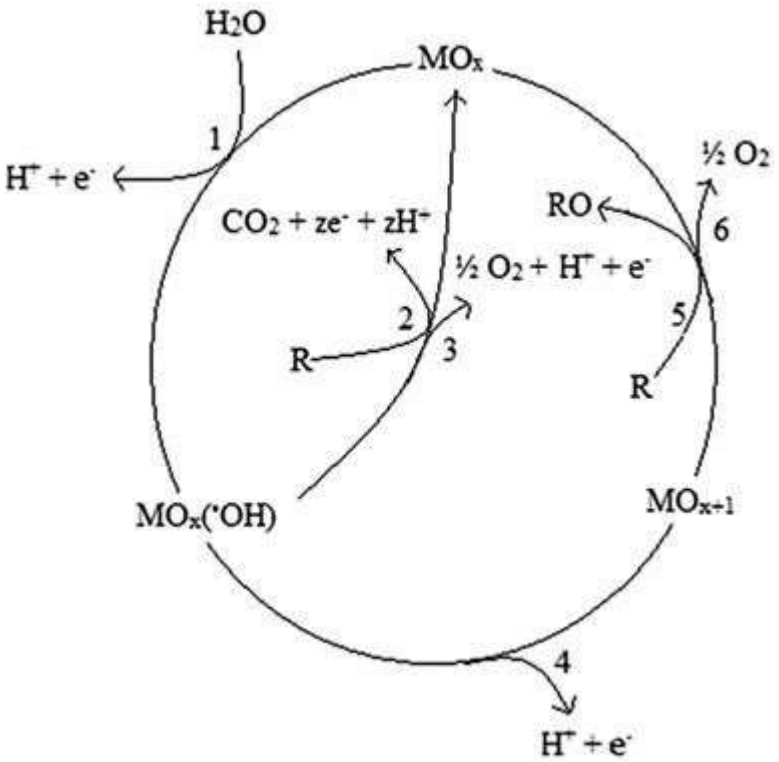

Scheme 2.1: Electrochemical oxidation of organics on metal oxide Adapted from Shestakova & Sillanpää (2017)

In the scheme 2.1, metal oxide semiconductor (MO x) anode in process 1 show the reduction of water molecules. Process 2 is the Combustion of R (organic molecule). Process 3 and 6 illustrates O_2 evolution, while process 4 indicates the formation of higher oxide. Process 5 is the conversion of organics, R to organic oxides, RO. Such is the indirect oxidation of organic species in an anode electrode.

Direct oxidation only occurs at the surface of the electrode when there is a direct exchange of electrons between the anode and oxidizable organic species at the interface. The degradation of the pollutants takes place when they diffuse and are adsorbed at the anode, or by active species adsorbed onto the anode surface (Rasalingam *et al.,* 2014). This oxidation takes place at low potentials, below the oxygen evolution overpotential. Nonetheless, the anode surface still undergoes passivation due to adsorption of organic

molecules (Subba Rao & Venkatarangaiah, 2014). The mechanism of oxidation of organics on metal oxide anodes as proposed by Shestakova & Sillanpää (2017) shows that hydroxyl ($\bullet OH$) radicals are generated on the anode surface by water discharge at high potentials. The ($\bullet OH$)radicals then adsorb physically or chemically on the metal oxide anode (MO_x) as shown in equations (2.1) and (2.2).

$$MO_x + H_2O \rightarrow (\bullet OH) + H^+ + e^- \quad (2.1)$$

$$(\bullet OH) \rightarrow MO_{x+1} + H^+ + e^- \quad (2.2)$$

In this study, chemisorption refers to the strong binding of oxygen species to the electrode surface forming higher-valent oxides, while physisorption describes the weak, reversible attachment of hydroxyl radicals on the electrode surface prior to oxidation of organic molecules. During electro-oxidation, hydroxyl radicals (•OH) generated at the anode surface interact with the electrode material to produce metal oxides of higher oxidation state (MO_{x+1}) in active anodes. Active electrodes therefore participate in surface redox chemistry, where the metal oxide lattice undergoes reversible oxidation, forming chemisorbed oxygen species (MO_{x+1}/MO_x). These chemisorbed oxygen species act as the primary active sites responsible for the selective oxidation of organic compounds Shestakova & Sillanpää (2017).

In contrast, non-active electrodes primarily act as electron sinks and provide minimal surface interaction with organics due to the absence of significant adsorption sites. After the initial chemisorption step, physiosorbed hydroxyl radicals on the electrode surface facilitate further oxidation of organic molecules, progressively converting them into CO_2 and H_2O, as illustrated in equations (2.3) and (2.4).

$$MO_x + \bullet OH + RH \rightarrow H_2O + R \quad (2.3)$$

$$\bullet OH + R \rightarrow MO_x + CO_2 + H_2O \quad (2.4)$$

It is notable that most electrochemical methods currently used for wastewater treatment are energy-intensive because they rely on conventional electrolytic cells, which require continuous external electrical input to drive non-spontaneous oxidation reactions. This makes their application at small-scale level economically impractical, particularly in decentralized or low-resource settings. Electrolytic systems consume energy rather than produce it, unlike fuel-cell-based electrochemical systems, which generate electricity from spontaneous redox reactions and therefore offer greater efficiency and sustainability for treatment and energy recovery applications.

In this work, a novel electrochemical approach that does not rely on external electrical energy was employed to oxidize organic matter in wastewater. The system instead generates its own potential to sustain the oxidation reactions, demonstrating a cost-effective alternative for small-scale water purification and promoting practical water recycling solutions.

2.5 Electrochemical cell in this work

This study adopted an electrochemical cell configuration inspired by MFC design to degrade oxidizable species dispersed in water. Unlike conventional MFCs, this system operates without microorganisms, thereby eliminating secondary pollution associated with biomass growth and sludge formation. The process is driven by solar energy rather than external electrical power, making it cost-effective and suitable for small-scale water purification applications.

The cell consists of an anodic chamber containing wastewater, which was continuously bubbled with air. Air bubbling ensured a continuous supply of dissolved oxygen to support

oxidation reactions and to replace the microbial role normally present in MFCs, thereby maintaining an oxidative environment for pollutant degradation. The anode material plays a critical role in determining the efficiency and selectivity of the electrochemical reactions (Sequeira & Santos, 2009), as it facilitates the generation of reactive oxidizing species through electron transfer processes analogous to metabolic oxidation in biological fuel cells.

Two different anode materials were evaluated in separate remediation reactors for in-situ generation of strong oxidizing species. One system employed a platinum anode, which exhibits electrocatalytic properties and promotes oxygen reduction reactions as reported by Huang *et al.* (2021). In this configuration, oxidation of organic matter proceeds via the electro-generated oxidizing species formed at the platinum surface shown in equations 2.5–2.7 (Cheng, 2015).

$$H_2O \rightarrow \bullet OH + H^+ + e^- \quad (2.5)$$

$$O_2 + 2H^+ + 2e^- \rightarrow H_2O_2 \quad (2.6)$$

The overall equation 2.7 is as shown.

$$O_2 + 2H_2O \rightarrow 2H_2O_2 \quad (2.7)$$

The second reactor configuration employed a dimensionally stable anode fabricated by modifying a graphite electrode with an iron (III)-doped titanium dioxide coating. In both reactor setups, a graphite electrode served as the cathode. This system utilized the electron-transfer characteristics at the interface of a stable anode surface to promote the degradation of oxidizable species. Graphite was selected because it does not react with water to form harmful by-products and is therefore suitable for long-term deployment in electrochemical systems (Reimers *et al.,* 2006; Bekyarova *et al.,* 2013; Shao *et al.,* 2018). In addition,

graphite possesses a delocalized π-electron network that facilitates efficient electron mobility, allowing it to function as an effective electron acceptor and conductive support during oxidation processes (Dumas *et al.,* 2007; Richter *et al.,* 2008; Yi *et al.,* 2009). This property enables electrons generated during oxidation of organic matter to be transferred efficiently, enhancing the electrochemical performance of the system.

In this configuration, the graphite electrode was coated by dip-coating with iron (III)-doped titanium dioxide to enable photo-oxidation of organic contaminants into harmless end-products. Titanium dioxide (TiO_2) has been widely used in wastewater treatment as a photocatalyst due to its chemical and biological inertness, non-toxicity, and cost-effectiveness (Al-Mamun et al., 2019). Doping TiO_2 with Fe (III) improves conductivity and reduces its band gap, allowing activation under visible light rather than UV alone (Gavali, & Thapa, 2021). Upon illumination with sunlight, TiO_2 generates electron–hole pairs: electrons are excited from the valence band to the conduction band, leaving behind positively charged holes. These charge carriers participate in redox reactions at the electrode surface, driving the oxidation of organic pollutants in wastewater as shown in equation 2.8 (Pathiraja *et al.,* 2014).

$$TiO_2 \xrightarrow{hv/moist} h^+ + e^- \qquad (2.8)$$

The resulting electrons move to the surface of the semiconductor, and reduce the oxygen and water molecules generating reactive oxidizing species, while the electron deficient holes increase the surface area for the oxidation process of the organics in water as shown in scheme 2.2.

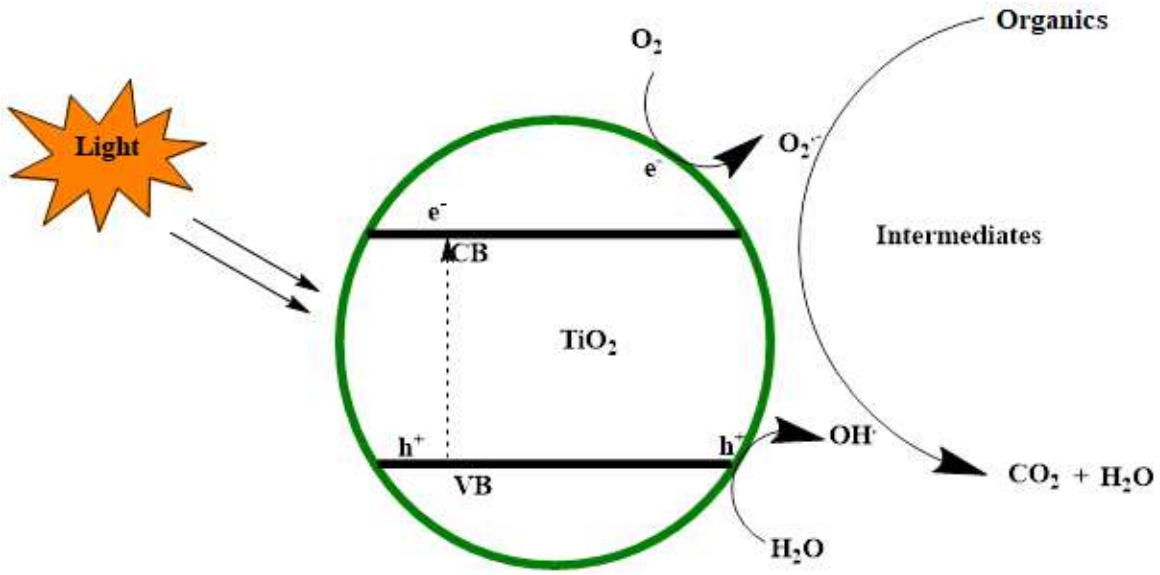

Scheme 2.2: The mechanism of titanium dioxide as a Photocatalyst in degradation of organic matter

The use of visible light from natural light as a clean energy was thus used to accelerate the oxidation process. This implies that in this technique, the reaction can only take place if an anode of an electrochemical cell is made to be photoactive. A photoactive anode in presence of light generates reactive species that speed up the oxidation of dissolved organic species in water (Miklos *et al.,* 2018). The dimensionless stable electrode, acted as a photocatalyst, hence used as an anode in the electrochemical cell to enhance the photo oxidation of organic species in the water. The electrons generated in both cases were conducted through an external conductor to the cathode and the protons pass through the proton exchange membrane (PEM) to balance the charges due to the electrons. The difference in potential between the two compartments of the cell resulting from the oxidation reaction that occurs boosts electrons' kinetic energy and enable them move to the counter electrode (Ibanez *et al.,* 2018). The electrons then migrate to the cathode due to the electromotive force.

The PEM used in this study was made from a conducting polymer inert in aqueous media. The materials used to make the PEM and the PEM itself are not soluble in water and as such it does not get incorporated in the water causing pollution. The separation of the two chambers ensured that there was no interaction between species in either of the chambers of the electrochemical cell. The wastewater was continuously bubbled through the anodic chamber to provide the required oxygen. This was to generate strong oxidizing species capable of oxidizing the DOM and eventually release water and carbon dioxide (Khotseng, 2018). The electrons released during that process, migrated from the anode to the cathode via an external conductor. The redox reaction is analogous to the corrosion process where there is a spontaneous oxidation of a metal by oxygen in the environment (Singh *et al.,* 2010).

The generated electrons in the anodic chamber make that compartment of the cell negatively charged and as such, the conductor immersed in that solution becomes a negative terminal (anode) of the cell. Via external conductors the anode to the cathode is connected while the solutions in the cell are separated by a membrane. This is because the protons diffused through the PEM due to the difference in the charges at the anode and cathode (Singh *et al.,* 2010).

The presence of an oxidizing agent or oxygen at the cathode recombines with hydrogen and the electrons from the anode to produce pure water, making this method efficient in its combustion process, hence reducing water pollution (Peter, 2018). Such a cell can be stationed at a domestic set up for wastewater treatment or at any other site where biomass immersed in water is plenty (Cano-Castillo, 2013).

2.6 The proton exchange membrane

A proton exchange membrane plays a critical role in electrochemical systems by selectively transporting protons while preventing the mixing of oxidizing and reducing species. It therefore supports charge balance and contributes to the conversion of chemical energy into electrical energy during water treatment. An ideal PEM should be chemically inert, mechanically stable, insoluble in water, and exhibit high proton conductivity with minimal internal resistance (Amado *et al.,* 2016).

Several PEM materials have been investigated in electrochemical and microbial fuel cell systems. For example, Ghasemi *et al.* (2015) prepared a sulfonated polyether ether ketone (SPEEK) membrane that achieved a maximum power density of 126.1 mW/m² in an MFC. Mokhtarian *et al.* (2013) developed a Nafion-polyaniline (PANI) membrane based on Nafion 112, which produced 124 mW/m², while Ghasemi *et al.* (2012) fabricated a doped PANI-polysulfone membrane that yielded 62.5 mW/m². Ceramic PEMs have also been explored; Midyurova *et al.* (2016) synthesized various clay-based membranes and applied them in sediment MFC systems, generating voltages in the range of 17.8–20.2 mV, demonstrating potential for low-cost alternatives.

Among these membranes, Nafion remains the benchmark due to its excellent proton conductivity and chemical stability (Logan *et al.,* 2006). However, it is costly, limiting its applicability in decentralized or small-scale treatment systems. SPEEK and PANI-based membranes provide moderate conductivity at a lower cost, while ceramic membranes offer low-cost and durable options but generally lower proton transport efficiency. Ultrex has also been explored as a commercial alternative to Nafion but still presents cost limitations (Ghassemi & Slaughter, 2017). Considering performance, cost, and environmental factors,

there remains a need for affordable and chemically stable PEMs for small-scale water treatment.

In this work, a conducting polymer synthesized from aniline was developed and employed as the PEM. The resulting PAni membrane, anchored onto a porous fritted glass support, served as an inert, water-insoluble, and chemically stable ion-exchange material capable of selectively transporting protons cost-effectively. It functioned passively by facilitating proton migration from the anode to the cathode, consistent with conventional proton-exchange behavior in electrochemical systems, while maintaining compartment separation without introducing secondary pollutants. The membrane was incorporated into a two-chamber electrochemical cell designed for the purification of domestic wastewater, where it provided effective ion transport and electrical continuity. The electrodes were externally connected to complete the circuit and initiate oxidative degradation of pollutants at the anode half-cell, while the cathode chamber was filled with 0.01 M potassium chloride solution to enhance ionic conductivity and improve the overall efficiency of the degradation process (Bond *et al.,* 2002; Tabassum *et al.,* 2021).

2.7 Polyaniline

Polyaniline is an organic conducting polymer that has been studied widely due to its low cost, simplistic ways of preparing and the ease of doping. It can be found in different oxidation states ranging from leucoemeraldine when fully reduced, protoemeraldine, emeraldine, nigraniline, and pernigraniline when fully oxidized. However, PAni conducts only when it is moderately oxidized (the emeraldine form). An easy method of doping polyaniline is by use of protonic acids, such as hydrochloric acid, sulphuric acid and phosphoric acids (Bienkowski, 2006).

The protonation takes place first at imine groups that contribute to a spinless charged bipolaronic structure, then rearranges to relatively stable radical cations followed by polaron separation in a polaronic structure with delocalized p-charge carriers and conjugated π-bonds. The doped PAni can be dedoped adding a base to the polymer which forms the emeraldine base form (Boddula & Srinivasan, 2014). Polyaniline can be synthesized electrochemically or chemically.

2.7.1 Aniline polymerization

Different mixtures of polyaniline in form of polymer matrix are conducive for a variety of applications. This is because the desired properties are easily achieved by varying the host polymer and reaction conditions (Sen *et al.,* 2016; Zeghioud *et al.,* 2015). Polyaniline is prepared through chemical polymerization by ammonium peroxydisulfate oxidation of aniline at a pH below 2.5. It is obtained as a precipitate salt of polyaniline hydrogen sulfate. During oxidation, a pair of electrons on nitrogen in the aniline monomer is removed. This creates positive polaron in the chain that causes deformation in the chain structure. As a result, the polyaniline structure has π-electron clouds overlapping above and below its structure. This provides for polyconjugate system which is a charge carrier system in the polymer. The content of oxidized nitrogen atoms in polyaniline can change from zero in its reduced form, leucoemeraldine to nearly one in the fully oxidized state, pernigraniline (scheme 2.3) (Sapurina *et al.,* 2015).

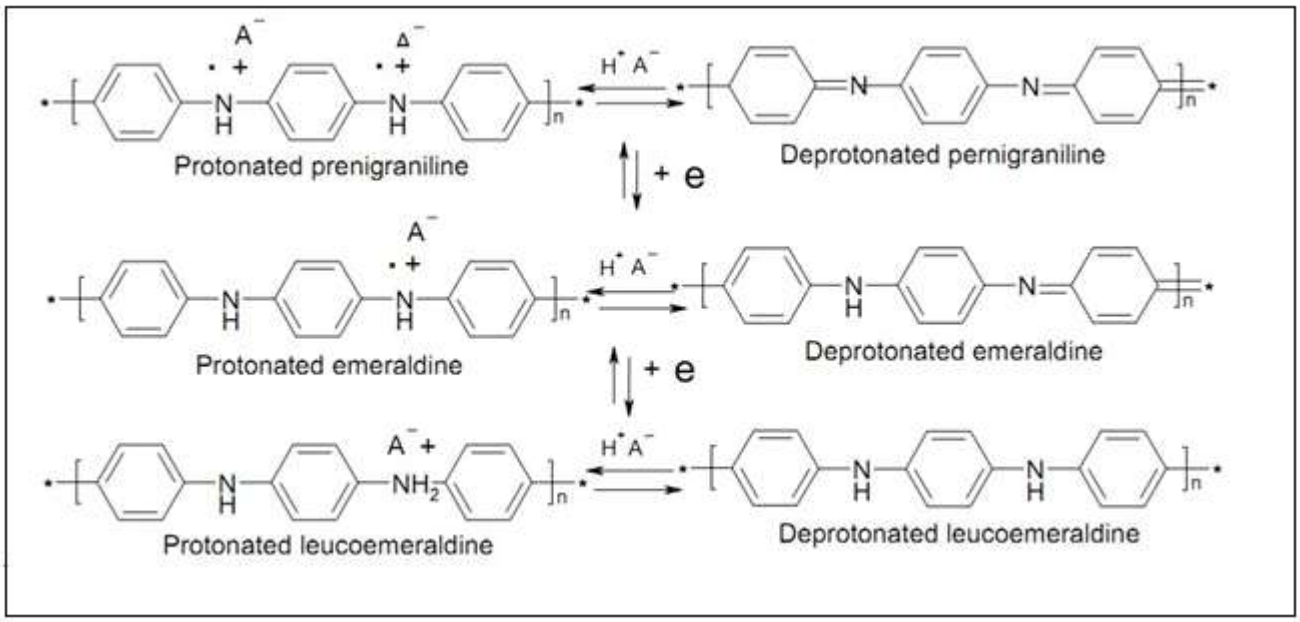

Scheme 2.3: Different forms of Polyaniline polymer

The most stable form of polyaniline is emeraldine, in which every second nitrogen atom is oxidized, and polymer chain contains equal number of oxidized and reduced units (Molapo *et al.,* 2012).

2.7.2 Mechanism of aniline polymerization.

Oxidative polymerization can be explained by electrophilic substitution reaction of aniline and oxidized nitrogen in another aniline molecule as shown in scheme 2.4 and 2.5.

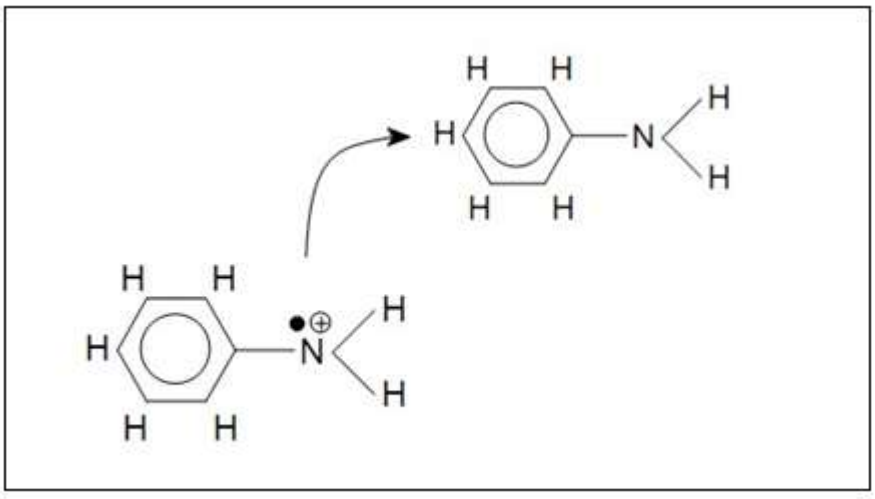

Scheme 2.4: Electrophilic substitution reaction

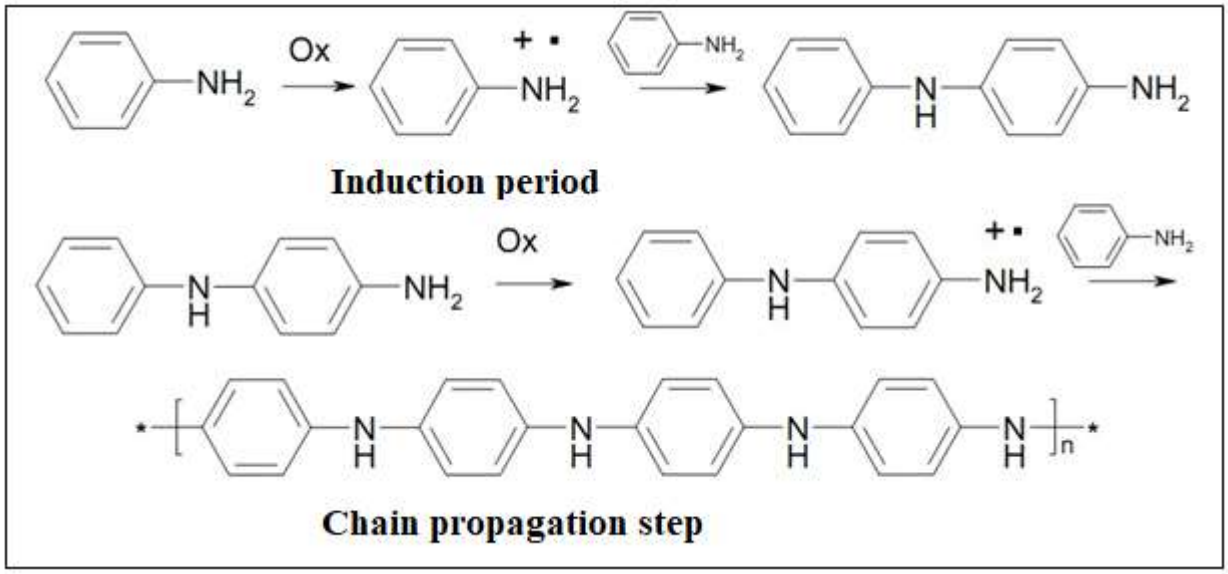

Scheme 2.5: Aniline oxidative polymerization process

In this case, the oxidized nitrogen acquires a positive charge to form an aniline cation radical. The radical then attacks the phenyl ring of another aniline molecule and substitute a proton from the ring. Both the ring and nitrogen in the aniline radical lose one proton. The monomer units then bind with each other, and the chain becomes longer. The polymerization process is terminated when one of the reactants, either monomer or the oxidant is depleted. The state of the end product depends on the strength of the oxidizing agent and the stoichiometric ratio of monomer to oxidant. If a strong oxidizing agent was used in excess, the end product is the pernigraniline and when polymerization is carried out under stoichiometric conditions or with excess aniline, emeraldine is the end product (Ćirić-Marjanović, 2013).

When polymerization takes place at a pH less than 2.5, the amino groups of the chains, and the monomers, are protonated. This maintains a balance of electron exchange between chain and monomer while all growth patterns other than *para*-substitution are forbidden.

This leads to the formation of regular polyconjugate chains of polyaniline with unique conducting properties and high molecular weight (Sapurina *et al.,* 2015).

2.8 Oxidation of Dissolved organic matter using Hydrogen peroxide

Dissolved organic matter, DOM is commonly defined as any organic substance that passes through a given filter of between 0.1 and 0.7μm (Denis *et al.,* 2017). The main components of DOM include carbohydrates, amino acids, proteins, phenols, lipids, alcohols, sterols and organic acids. When DOM undergo degradation, it produces products such as dissolved inorganic carbon (DIC), CO, CH_4, CO_2, and low molecular weight organic acids (Ward & Cory, 2016). The degradation of DOM can be photo induced or initiated by the presence of oxidizing agents. In both cases, the formation of reactive oxidizing species such as super oxides and hydroxyl radicals are responsible for the degradation process.

Hydrogen peroxide is a suitable oxidizing agent that is stable but reactive. It undergoes photo decomposition to generate radicals (hydroxyl) which have strong oxidizing properties that indirectly initiates oxidizing reactions of DOM in water. Hydrogen peroxide radicals react with DOM in water to completely mineralize them to carbon (IV) oxide and water as the degraded product in equation 2.9).

• $2HO + DOM \rightarrow CO_2 + H_2O$ (2.9)

The redox equations for the domestic wastewater have been proposed by (Ike *et al.,* 2019; Koroglu *et al.,* 2019) and are presented in equations 2.10 and 2.12.

Oxidation of domestic wastewater (at the anode)

$$C_{10}H_{19}O_3N + 18H_2O \rightarrow 9CO_2 + NH_4^+ + HCO_3^- + 50H^+ + 50e^- \quad (2.10)$$

Reduction equation (at the cathode)

$$O_2 + 4H^+ + 4e^- \rightarrow 2\,H_2O \quad (2.11)$$

The overall equation

$$2C_{10}H_{19}O_3N + 27O_2 + 8H^+ \rightarrow 18CO_2 + 2NH_4^+ + 2HCO_3^- + 18H_2O \quad (2.12)$$

2.9 Previous studies on *in-situ* electro-oxidation of dissolved organic substances

Previous studies on *in-situ* electro-oxidation of dissolved organic substances has been reported by (Ryan *et al.,* 2021) as they evaluated sequential electro-coagulation and electro-oxidation processes for *in-situ* removal of trace organic compounds (TOrCs), acyclovir (ACY), trimethoprim (TMP), and benzyl dimethyl decyl ammonium chloride (BAC-C10) in model ground and surface waters. The sequential process registered a removal efficiency of 74 ± 7% for dissolved organic carbon from model surface water. Despite the success of the process, it was reported that the removal of those dispersed species was energy intensive. This therefore had a challenge and thus limits the upscaling of such a technology. Another *in-situ* remedial process was reported by (Pei *et al.,* 2020) as they developed organic Fenton-like catalysis using redox-active polymeric intermediates. In this work, phenol was degraded with production of both oxygen and hydroxyl radicals in the anodic phenol conversion using the in-situ organic Fenton-like catalysis. However, this system contained quinone like moieties and persistent organic radicals which are pollutants of concern in the treated waters.

An *in-situ* radical and non-radical oxidative degradation of organic compounds in complex real matrix was carried out by (Ganiyu & El-Din, 2020). In that work, the electrolysis of oil sands process water was carried out using boron doped diamond electrode. That method achieved

complete mineralization of dissolved organic contents at current density ≥ 5 mA cm^{-2}. However, this was also an energy intensive process that required enormous quantities of energy and therefore expensive in the long run. To overcome such challenges, this study developed an electrochemical method, effective in degradation of organic pollutants and does not require external form of energy to drive it.

2.10 Cost Effectiveness of Wastewater Treatment Methods

The cost of wastewater treatment is a major factor influencing the adoption and sustainability of purification technologies, particularly in low-resource settings. Conventional treatment methods such as coagulation, chlorination, and membrane filtration are often associated with high operational and maintenance costs due to chemical consumption, sludge handling, and energy requirements (Chen *et al.,* 2019; Ganiyu *et al.,* 2018). Biological systems, including microbial fuel cells and activated sludge processes, have been explored as cost-effective alternatives; however, their dependence on microbial activity results in long start-up times, strict environmental control, and high maintenance, which reduce their overall economic viability (Liu *et al.,* 2020; Logan *et al.,* 2019). Similarly, electrochemical and advanced oxidation processes achieve high degradation efficiencies but are limited by the cost of sacrificial electrodes, use of external oxidants such as hydrogen peroxide, and significant energy consumption (Martínez-Huitle & Ferro, 2016; Ganiyu *et al.,* 2020). To address these challenges, recent research emphasizes the development of sustainable electrochemical systems capable of generating reactive oxidative species in-situ without added reagents or sacrificial materials, thereby lowering operational costs and enhancing scalability (Woo *et al.,* 2020; Garcia-Segura *et al.,* 2021). The electrochemical approach proposed in this study builds on this concept, aiming to provide an efficient, low-cost, and environmentally friendly solution for point-of-use wastewater treatment.

2.11 Characterization

The synthesized polymer, iron doped titanium oxide and modified electrode are characterized using several analytical techniques to determine their structural, morphological, optical, and electrochemical properties and to confirm polymer identity and transformation during degradation.

The Scanning Electron Microscopy (SEM) coupled with Energy-Dispersive X-ray Spectroscopy (EDX) examines the surface morphology, particle distribution, and elemental composition of the iron doped titanium oxide. SEM scans the sample with a focused electron beam and generates high-resolution images that reveal particle size, porosity, agglomeration behavior, and surface texture (Saif *et al.,* 2017). The EDX simultaneously detects characteristic X-rays emitted from the sample, allowing identification of titanium, oxygen, and dopant metals and confirming successful metal incorporation into the TiO_2 matrix (Paul, 2018). The X-ray Diffraction (XRD) determines the crystalline phases and structural characteristics of the iron doped titanium oxide. The technique records diffraction patterns resulting from the interaction of incident X-rays with atomic planes in the crystal lattice. The diffraction peaks are compared with standard reference patterns to identify anatase and rutile phases of TiO_2. Peak shifts and broadening provide evidence of lattice modification due to doping and allow estimation of crystallite size using the Scherrer equation (Khan *et al.,* 2020).

The UV-Visible spectroscopy evaluates the optical absorption properties and electronic band structure of the iron doped titanium oxide. The instrument measures light absorption across the UV-Visible range, and the band-gap energy is calculated using Tauc plots. Shifts in the absorption edge and decreases in band-gap values indicate enhanced visible-light absorption

and improved photoactivity potential arising from metal modification (Zedek *et al.,* 2021). Fourier Transform Infrared Spectroscopy (FTIR) identifies the chemical structure and functional groups of the polymers. The technique measures infrared absorption corresponding to specific molecular vibrations, enabling polymer identification.

Potentiometric characterization evaluates the electrochemical behavior of the modified DSA. The technique measures the potential difference between the working and reference electrodes under open-circuit conditions. Measurements under both dark and illuminated conditions assess photo-responsiveness and surface charge behavior. A shift in potential upon illumination indicates photo-induced charge carrier generation, while stable potential values confirm the suitability of the electrode for electro-oxidation and photocatalytic wastewater treatment applications (Carbonari *et al.,* 2017).

2.12 Research gap

Although biological treatment systems such as microbial fuel cells demonstrate high efficiency in removing dissolved organic pollutants from wastewater, their reliance on microbial activity presents several limitations. These include slow start-up times, the need for specific electrochemically active bacteria, potential release of microorganisms into treated water, use of toxic and costly mediators in some systems, and operational instability under varying environmental conditions. Existing chemical and electrochemical approaches, including electrocoagulation and advanced oxidation processes, are effective but generate secondary chemical pollution, sludge, require sacrificial electrodes, or depend on externally supplied oxidants such as hydrogen peroxide, increasing cost and operational complexity. Despite

advances in wastewater treatment technologies, there is limited research on electrochemical systems that can generate reactive oxidative species *in-situ* and degrade dissolved organic pollutants without microorganisms, sacrificial electrodes, added reagents, or secondary pollution, particularly for point-of-use domestic wastewater treatment.

This study addresses this gap by developing and evaluating a microbe-free electrochemical cell inspired by MFC design, capable of producing oxidizing species internally while simultaneously oxidizing dissolved organic matter. The approach aims to provide a sustainable, chemical-free, low-sludge, point-of-use purification solution suitable for water-scarce environments.

CHAPTER THREE

MATERIALS AND METHODS

3.1 Research design

This study involved several steps in its design. First, conducting polymeric material was synthesized in the laboratory and characterized. Next, a membrane material was prepared from this synthesized polymer. A dimensionally stable anode was a graphite rod modified by dip coating it in paste of iron (III) spiked titanium dioxide. Following that, components of an electrochemical cell were assembled using a glass blowing procedure to create the reactor vessel for the electro-oxidation process in this investigation. The redox kinetics was monitored in the remediation of dissolved organic species using synthetic wastewater. Finally, the assembled cell was employed in treating actual domestic wastewater. The flow chart of the process is shown in figure 3.1

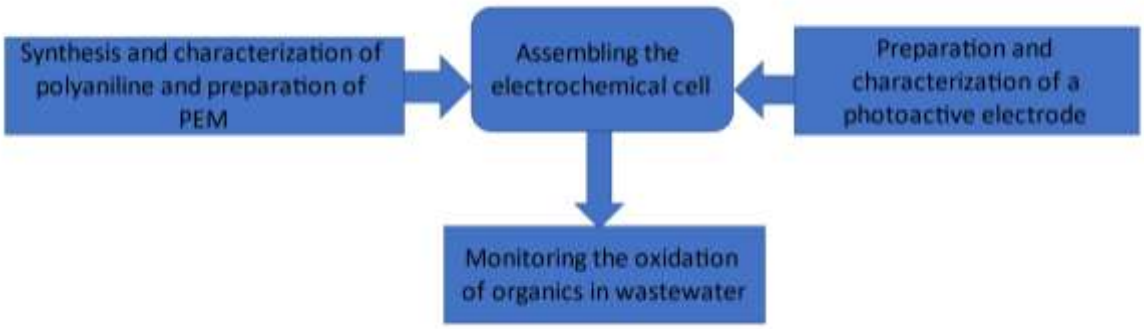

Figure 3.1: Research methodology flow chart

3.2 Materials and reagents

All solutions in the entire study unless otherwise stated were dispersed in double distilled water and all the reagents used were of analytical grade. Aniline, starch, potassium iodide, iodine, hydrochloric acid, potassium persulphate, potassium chloride, phosphorus oxide, polyvinyl alcohol, calcium silicate, Degussa P25 titanium dioxide, Iron (III) chloride, Iron (III) nitrate, polystyrene and sulphuric (VI) acid were all from Sigma-Aldrich chemicals

supplied by Kobian which its outlet in Nairobi, Kenya. Both the graphite electrode (5.0 mm diameter and 5 cm length) and the platinum electrode (0.45 mm diameter and 7.0 cm height, 99.9% trace metals basis) were also supplied by Sigma-Aldrich. A Rocker pump model Chemker 410 was used to circulate the water and bubble air in the anode compartment of the reactor (cell) during the experiment.

3.2.1 Preparation of starch solution

Starch solution was prepared where soluble starch was dissolved at a ratio of 1.0g per 100 mL of distilled boiling water. This solution was then delivered into the anodic chamber as the wastewater sample. Normal starch stock solutions for formulating a calibration curve were prepared to produce 0.01%,0.02%, 0.05%, 0.10%, 0.15%,0.20%,0.40% and 0.50% starch solutions. Iodine solution was used in the absorbance measurements of starch solution during degradation.

3.2.2 Preparation of iodine solution

A standard iodine solution (0.05 M) was made by dissolving iodine (7.0 g) and potassium iodide (18.0 g) in distilled water (100 mL). Afterwards, 3 drops of hydrochloric acid were added and then the solution was diluted to make it to a litre. The resultant solution was then poured into an opaque bottle.

3.3 Apparatus and Instrumentation

A magnetic stirrer with hot plate was used for controlled polymerization of aniline, with acidity monitored using a pH meter. An analytical balance ensured accurate weighing of reagents, while glassware such as beakers and volumetric flasks supported solution preparation and washing steps. The polymer membrane and electrode coatings were dried

in a laboratory oven, and a porous glass frit served as a casting support. A muffle furnace was used for calcination of titanium precursors, and a freezer was used for storage of temperature-sensitive solutions.

Material characterization employed a UV–Visible spectrophotometer to assess optical properties, and a Fourier Transform Infrared spectrophotometer (Perkin Elmer 100, ATR mode) to identify functional groups in the polymer membrane. Surface morphology and elemental composition of the electrode coating were examined by SEM-EDX (ZEISS), while crystallinity of iron-doped TiO_2 was confirmed using XRD (RUKAGU Corp., Tokyo, Japan). Electrical conductivity of the membrane was measured using a Fluke 115 True-RMS multimeter, and electrochemical characterization of the dimensionally stable anode (DSA) was carried out using a BASi Epsilon potentiostat with Ag/AgCl reference and platinum counter electrodes.

The electrochemical cell comprised a 250-mL borosilicate glass reactor fitted with a Fe–TiO_2 coated DSA (5.0 cm × 6.0 mm), a platinum electrode (70.0 cm × 0.45 mm) for comparative studies, and a graphite cathode. The system was connected using insulated wires, with circuit monitoring by digital multimeter. A Chemker 410 rocker pump circulated the model wastewater and aerated the anode chamber. Degradation kinetics were monitored periodically by UV–Visible spectrophotometry, with timed sampling performed using micropipettes, sample vials, and a stopwatch. Physico-chemical water quality parameters were further analyzed using a Palin Test Photometer 7100 (Dubai, UAE).

3.4 Experimental setup

This study adapted the design of an MFC to create a cell capable of breaking down oxidizable substances present in water within the anodic chamber, without relying on microorganisms (Rahimnejad, 2023). Instead, the concept proposed the use of an electrocatalytic and/or a photocatalytic electrode as the triggering material for the oxidation process at the anode. The anodic chamber was aerated to initiate the redox reaction. A conducting polymer that is inert and less expensive was also prepared from aniline for use as a proton exchange membrane in the cell. The oxidation of organic species in wastewater was facilitated by production of oxidizing species on the surface of the anode electrode within the electrochemical cell through an electron transfer process similar to typical metabolic pathways. This integration occurred when the wastewater treatment system was incorporated as a component of an electrochemical cell, illustrated in figure 3.2.

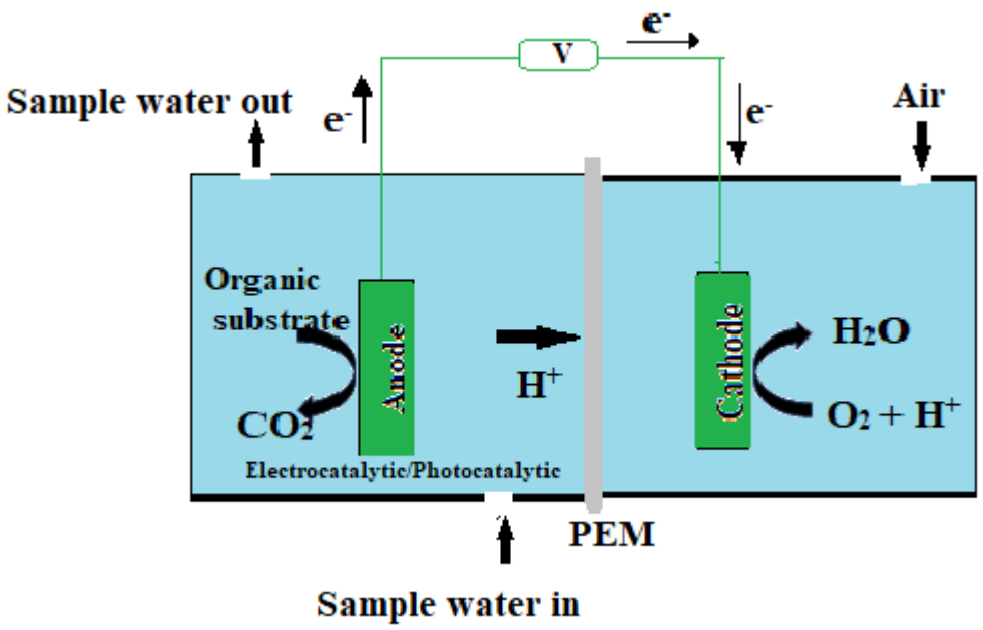

Figure 3.2: The experimental setup of the assembled electrochemical cell

The figure 3.2 highlights a crucial element of the electrochemical system: the anode electrode, where the conversion of organic contaminants into carbon dioxide and water

occurs. The material composing the anode significantly influences the efficiency and selectivity of the electrochemical process at this site (Sequeira & Santos, 2009).

3.5 Components of the electrochemical cell

3.5.1 The Proton Exchange membrane

The proton exchange membrane was an assembly of several components which consisted of a hydrogel, synthesized polyaniline, binder and a porous glass flitz.

3.5.2 Preparation of a biomass-hydrogel

A hydrogel material was prepared to seal the pores on the final PEM material to prevent migration (leakage) of water from the anodic to the cathodic chamber or vice versa. It also hydrated the membrane to enhance its conduction property (Gebel, 2000). The procedure for the preparation was according to Mwangi and co-workers (Mwangi *et al.,* 2019) as they modified cow dung to form material with high water retention capacity. The resultant material was dried at 60.0 ˚C and 2.0 g of that dry material was used in the preparation of the conducting polymer membrane.

3.5.3 Polymerization of the conducting polyaniline

This was done by introducing distilled aniline (200 mL) into a reactor and then adding 2.0 M hydrochloric acid (300 mL). The mixture was stirred for 30 minutes. In a separate connical flask, potassium persulphate (36.0 g) was dissolved in 2.0 M hydrochloric acid (200 mL). The persulphate solution was added to the aniline, and the resultant solution was mixed with the biomass hydrogel (2.0 g) and stirred thoroughly to form the conducting polyaniline polymer.

3.5.4 The assembly of proton exchange membrane

The exchange membrane was prepared as reported by Huang *et al.* (2016). Polyvinyl alcohol (6.0 g) was added to distilled water (100 mL) under heating while stirring to dissolve it for 2 hours. The resulting solution was then cooled to room temperature. It was then mixed with the previously prepared polyaniline (10.0 g), hydrogel (2.0 g) and calcium silicate (5.0 g) while constantly stirring to a uniform consistency. This product was frozen for 24 hours, and later thawed for 24 hours. It was then immersed in distilled water for 24 hours to remove inorganic impurities. The material was then analyzed using FTIR and then casted on the glass as a membrane for the cell.

3.5.5 Electric circuit continuity of the membrane

The continuity of the prepared membrane was determined as reported by Lu *et al.* (2019), using a Fluke 115 True-RMS digital multimeter (Singapore). This was done following a two-disk method (Amer & Young, 2013). The schematic presentation of the basic parts of the tester (multimeter) that was used for testing continuity tests across the test material is shown in figure 3.3.

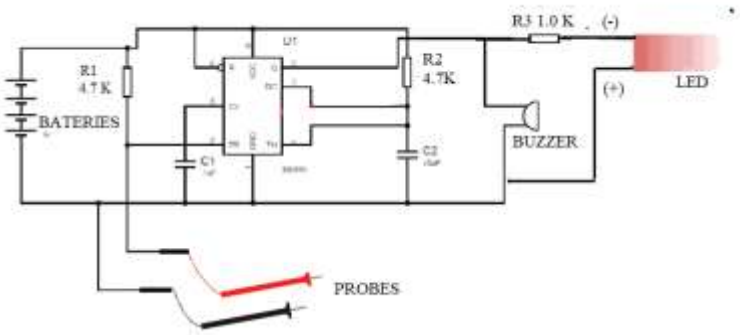

Figure 3.3: Schematic presentation of a continuity tester

By touching the negative and positive probes of the multimeter on the prepared polyaniline, both light from the LED and a buzz confirmed continuity. The polymer surface exhibited conductivity that was observed to be lower than 1 X 10^{-8} S cm^{-1}.

3.5.6 Fourier Transformed Infrared spectrophotometer on polyaniline

The Fourier Transformed Infrared spectrophotometer with attenuated total reflectance (ATR) mode (Perkin Elmer 100 with sampling accessory-Waltham, (MA, USA) was used to determine the functional groups of the prepared polyaniline polymer (Mukamel, 2000). A mass (0.1g) of the sample was used to make potassium bromide pellet using a pellet that was then analyzed in the mid-IR (4,000 – 400 cm^{-1}) region.

3.6 Anode of the electrochemical cell

This research employed two types of anodes in separate remediation reactors to facilitate the *in-situ* generation of strong oxidizing species for wastewater treatment. The first system utilized a platinum electrode, which is an electrocatalytically active material capable of supporting rapid oxygen reduction reactions without external activation, as reported by Huang *et al.* (2021). The platinum electrode (70.0 cm height, 0.45 mm diameter) operated under standard electrochemical conditions where oxidation occurred at the anode through electron transfer processes inherent to platinum's catalytic surface.

In contrast, the second setup used a dimensionally stable modified graphite electrode coated with iron (III)-doped titanium dioxide. Unlike platinum, this electrode functions as a photo-active anode, relying on light-induced charge separation within the TiO_2 layer to generate reactive oxidative species. Therefore, this configuration required different operating conditions—particularly illumination and aeration—to activate the photocatalyst and enhance electron transfer efficiency. The photo-electrode measured 5.0 cm in height and 6.0 mm in diameter. In both systems, a graphite electrode served as the cathode.

3.6.1 Modification of the graphite electrode

The graphite electrode (anode) in this study was modified by coating it with iron doped titanium dioxide. The iron-doped titanium dioxide was prepared by impregnation method (Amorós-Pérez *et al.,* 2018). To a sample of Degussa P25 titanium dioxide powder (5.0 g), 1 mL of 0.1 M Fe $(NO_3)_3$ solution was added. The resulting mixture was stirred for 2 hours and sonicated for 30 minutes. Subsequently, excess solvent was removed by drying the mixture in an oven at 80 °C for 24 hours. The sample was further calcined at 500 °C for 2 hours. This process aimed to decompose nitrates, eliminate impurities, and enhance the interaction between metal and TiO_2. The resulting powder was mixed with calcium silicate powder to the ration of 5:1 respectively in a 250 mL beaker. Distilled water (100 mL) was then added to the mixture and the mixture sonicated for 10 minutes to form a paste. The graphite rods were then (immersed) dipped into this paste for 24 hours and then air dried for 2 hours at first and then oven dried for 24 hours at a temperature of 80 °C. The dried rods were stored under water for 24 hours before use. This hydration step stabilizes the coating, improves adhesion, allows swelling and settling of the composite film, and prevents layer cracking or flaking when placed in service. It also removes any loosely

attached particles, ensuring a uniform, durable, and electrochemically stable electrode surface.

3.6.2 Characterization of the photoactive material

The effect of doping was investigated using a UV–Vis spectrophotometer. The equipment had an integrating spheres assembly that enabled the measurement of the total radiation reflectance and transmittance from the sample. This was to confirm the shift in frequency of excitement. A Shimadzu UV-2450 (Tokyo, Japan) UV–Vis spectrophotometer was used to confirm doping of titanium dioxide. A small sample (0.1g) of the iron doped titanium dioxide powder was placed in the powder kit and spectra reflectance measurements were carried out. Scanning electron microscopy (SEM: ZEISS microscopy) was used to examine the microstructural properties and Energy-dispersive X-ray (EDX) spectroscopy was used to determine the composition of the material. X-ray diffraction (XRD) (RUKAGU Corp. Tokyo Japan) was used to determine the crystalline phase and structure. A sample (10.0g) of the iron doped material was crashed using mortar and pestle. It was then placed in the sample holder and the phase was analyzed using radiation from CuKα (λ= 1.5406 Å).

3.6.3 Voltametric analysis

The voltametric analysis was divided in two sections. The first one was to characterize the graphite electrode to establish its performance upon modification using iron (III) doped titanium dioxide and second was for monitoring the variation of the oxidizable species in the anode compartment of the electrochemical cell. The equipment used is an Epsilon electro analyzer that is equipped with a door that can shield the analytes from external radiation as shown in the figure 3.4.

Figure 3.4: Epsilon electro analyzer equipped with a door used in the voltammetry analysis in this work

3.6.4 Characterization of the graphite electrode

The electrochemical effect of modification of the graphite was carried out because the anode electrode in the electrochemical cell has a high influence on the efficiency and the selectivity of the electrochemical process (Sequeira & Santos 2009). The electrochemical properties of the photoactive electrode were investigated by use of domestic wastewater analyte prepared as described in section 3.9.3. The analyte was supported in KCl 0.1 M and analyzed using the cyclic voltammetry. The experiment was undertaken at a scan rate of 100 mV/s on the modified electrode. The electrochemical analyzer was an Epsilon potentiostat (E2) with a cell stand Basi C3 (Dubai) using platinum electrode as a counter electrode and Silver/Silver chloride as reference electrode. These experiments were done at room temperature of about 25 °C, both in the dark and under natural light.

3.7 Monitoring the variation of the oxidizable species in the anode compartment

The voltametric analysis was also carried out to monitor the variation of the oxidizable species in the anode compartment of the electrochemical cell. The measurements were done using 0.1

M potassium chloride (pH 7.24) as the support electrolyte in which the analyte samples were dispersed. The solution was taken into the polarographic cell and continuously a voltammogram obtained to check the purity of the solution while purging with nitrogen gas. This was followed by addition of domestic wastewater sample solutions (5 mL) and a voltammogram obtained while the modified electrode was the working electrode and the cell was under visible radiation conditions. The process was repeated while the cell was not exposed to light. The results obtained were captured and recorded using a voltammeter

3.8 Assembling the electrochemical cell

A glass H-design cell with two chambers whose capacity is 250 mL on either side of the half-cell was assembled. A sintered glass disc (fritz), on which the ready PEM material was casted, was used to separate the two chambers, The slurry method was used to perform the casting (Goral *et al.,* 2009), where the prepared hydrogel polymer (10.0 g) was weighed before adding calcium silicate (1.0 g), distilled water (100 mL) and polyvinyl alcohol (2 mL). The mixture was rigorously stirred to form a suspension.

The cell was placed vertically and the mixture drained from one chamber to settle down at the frit to a 2.0 mm level. Using a strong suction pump, the solvent (water) was drawn from the opposite chamber to allow the packing material to settle solidly and clog the pores of the sintered glass fritz. This membrane was left to cure for one and a half days and the same procedure replicated for the other chamber. The hydrogel's volume increased after contact with water, ensuring that all the pores were clogged and hence the solutions between the two compartments could not mix.

The cell is a continuous flow reactor where the sample water is being continuously circulated from a reservoir (2 L) through the electrochemical reactor cell and back to the reservoir. The fabricated electrochemical cell assembled for this study is as shown in figure 3.5.

Figure 3.5: The assembled electrochemical cell in this study

A H-design electrochemical cell made of glass with two chambers with a capacity of 250 mL on each side of the half-cell was assembled. The chambers are separated by a sintered glass disc (fritz) on which the prepared PEM material is casted. The anode solution, where oxidation takes place is circulated with domestic wastewater containing dissolved organic matter using a peristatic pump to allow air bubbling to aid in the oxidation process. The solution in the cathodic chamber is kept constant. In one set of experiments, a platinum wire was used as the anode while graphite was used as the cathode. In another set of experiments, the iron-doped titanium dioxide coated graphite electrode which is the DSA was used as the anode in both set of experiments a graphite electrode was used in the cathode compartment.

3.9 The working of the cell

Starch solution (wastewater 2 litres) was circulated in one of the chambers (anode) via a water pump at a the rate of 18 L/min over the entire period of the experiment and the potential difference at the electrodes of the electrochemical cell was measured by a digital multimeter

(Fluke 115 True-RMS, Singapore). Distilled water containing dissolved potassium chloride (0.2 M KCl) was filled in the opposite cathode chamber. A platinum electrode was used as the anode while graphite was used as the cathode. Copper conductor was used to externally connect the anodic and cathodic chambers and the potential difference measured.

3.9.1 The anodic solution

The anodic solutions used in this cell were starch solution prepared as synthetic wastewater and green leafy vegetables solution as real domestic wastewater.

3.9.2 Measurements of degradation of starch in water

Aliquots of the starch solution (5 mL) were extracted at constant time intervals of 10 minutes for an hour. A drop of iodine solution was added to each of these samples, and then a UV-Vis analysis was done with the wave band range of 200 nm to 700 nm before recording absorbance readings for the region of maximum absorbance (λ_{max}). The potential difference across the electrodes was monitored using a digital multimeter and the voltage was recorded at constant time intervals.

3.9.3 Domestic wastewater

The domestic wastewater in the electrochemical treatment process was carried out using a solution obtained from the leaves of the normal green vegetables used in the kitchen for preparation of a meal. This solution was prepared by weighing chopped green leafy vegetables (9.0 g) and to that, distilled water (200 mL) was added and allowed to boil for 15 minutes, then cooled to room temperature. This solution was filtered to remove any suspended particles and then diluted to make it to 2 litres. This method was adopted to mimic the organic load typically found in domestic wastewater, particularly the biodegradable organic fraction originating from kitchen effluent and food preparation

residues. The use of vegetable extract as a model wastewater allowed for a controlled and reproducible organic content while representing real household wastewater characteristics, ensuring safe handling and eliminating variations that may arise from real wastewater sources. Samples of the prepared solution were then introduced into the electrochemical reactor similarly to the starch solution in the previous section and the potential difference monitored at regular time intervals. The analysis of the physio-chemical parameters of this water was also measured using a Palin test Photometer 7100, Dubai, United Arab Emirates.

3.9.4 The cathodic solution

Preparation of the cathodic solution was done by dissolving KCl (0.7 g) in a litre of distilled water. This ensured improved conductivity of the distilled water. The resultant solution had a temperature was 27 °C and a pH of 6.6.

3.10 Optical analysis of transparency of water

Visual analysis of the degradation of the dissolved organic matter in the sample of water was carried out by drawing wastewater samples (5 mL) from the anode compartment at regular time intervals of 30 minutes. The level of degradation was observed using an UV-Vis instrument at a wavelength ranging from 200 nm to 600 nm.

3.11 Optical analysis of the oxidation of dissolved organic matter

The degree of oxidation was analyzed using the starch iodine complex technique. This entailed drawing wastewater samples (5 mL), and then adding a drop of iodine solution. The mixture was then activated in a water bath at 70 °C for 2 hours to form starch iodine complexes. The samples were allowed to cool to 25 °C then analyzed on a UV-Vis spectrophotometer. The UV-Vis analysis was carried out within the wave band range of

200 nm to 700 nm and absorbance readings recorded for the region of maximum absorption (λ_{max}). The absorption data was fitted into first and second-order expressions to understand the degradation kinetics of the redox reaction taking place in the electrochemical cell. The same procedure was followed for the domestic wastewater only without the iodine complexation step.

3.12 Variation of oxidizable species in the oxidation process

Samples (5 mL), from the anode compartment were drawn every half an hour for 3 hours. A potentiostat was used to analyze the samples where cyclic voltammetry was done on the samples using platinum electrode as the functional electrode and Ag/AgCl electrode as the electrode of reference. The scanning rate used was 100 mV with a maximum current of 100 mA. One drop of the water sample solution was dissolved in 1.0 M KNO_3 solution (25 mL) which served as the supporting electrolyte. The experiments were conducted at room temperature of approximately 25 °C.

Differential Pulse Anodic Stripping Cyclic Voltammetry (DPASCV) was employed in this study to monitor the electro-oxidation progress. This hybrid electroanalytical technique combines features of differential pulse voltammetry and anodic stripping analysis with conventional cyclic voltammetry. In this method, analytes in the wastewater first undergo a pre-concentration step on the electrode surface, followed by a potential sweep where the accumulated species are stripped (oxidized) while recording current response.

The differential pulse component enhances sensitivity by applying small potential pulses during the scan, allowing detection of changes in redox behavior with greater resolution. This approach was selected because it provides high sensitivity to changes in electroactive organic

species and intermediates, enabling real-time monitoring of oxidation efficiency and electron-transfer dynamics during wastewater treatment. The electro-oxidation process was monitored using a potentiostat (Basi Epsilon, version 2.13.77) for the cyclic voltammetry (CV) measurement. Having detailed the materials, experimental procedures, and analytical techniques employed in this study, the next chapter presents and interprets the findings obtained.

CHAPTER FOUR

RESULTS AND DISCUSSIONS

4.1 Introduction

This chapter reports on the results obtained from all the experimental data obtained in this study. The results are discussed according to the order they appear in the experimental methods. They provide evidence for the deductions and conclusions made in the study. They include the synthesis and characterization of a conducting polymer from aniline, after which the conducting polymer was used in the preparation of a proton exchange membrane used in the assembly of the electrochemical cell. The chapter also highlights the preparation of a photoactive electrode for use in the oxidation process of dissolved organic matter in water. The results of the oxidation of dissolved organic matter in the laboratory using starch solution and the degradation of dissolved organic matter from green leafy vegetable solution using the cell are also presented here.

4.2 Characterization of the polymeric conducting membrane

The polyaniline conducting polymer used to cast onto a porous glass fritz was characterized using a Perkin Elmer 100 instrument Fourier Transform Infrared Spectrometer (FTIR) on the ATR mode and the results obtained are shown in figure 4.1.

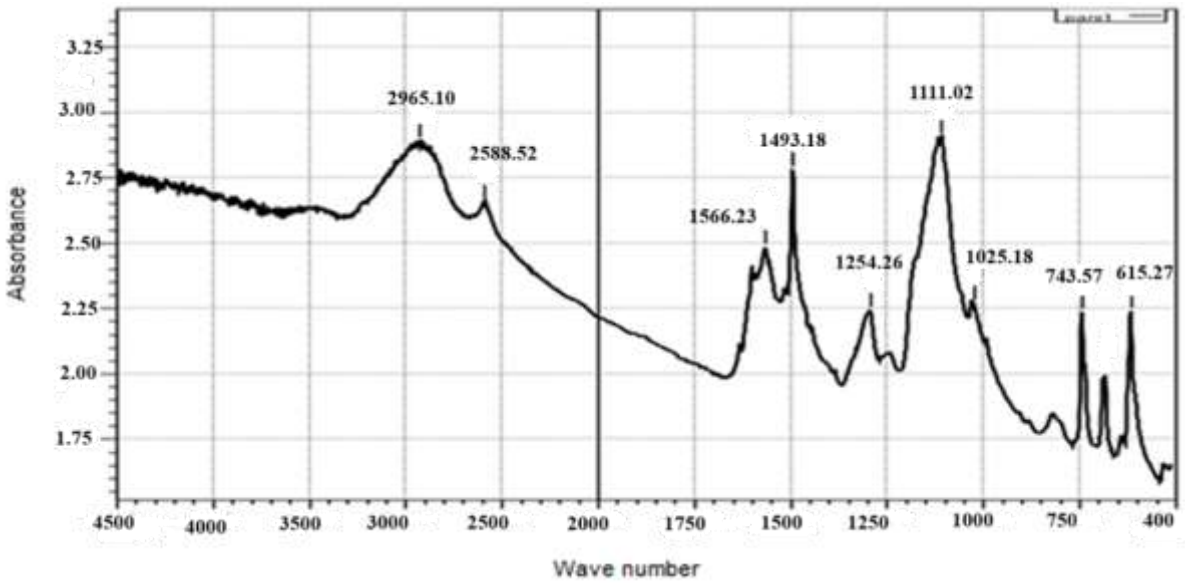

Figure 4.1: FTIR spectra of the synthesized conducting polyaniline polymer

The broad bands ranging 3200-2800 cm^{-1} were assigned to N-H stretching vibrations and C-H vibrations in the polymer (Kadari *et al.,* 2017). The peaks at 1566 cm^{-1} and 1493 cm^{-1}, were attributed to C=C stretching vibrations within the polymer that gives the polymer the conducting properties (Jamadade *et al.,* 2010). After confirmation of the structure, it was mixed with polyvinyl alcohol and calcium silicate as binder to make the membrane. It was then employed as a proton exchange membrane in the electrochemical cell and the degradation of the starch sample was then analyzed.

The conductivity of the membrane was confirmed by use of continuity tester whose light bulb glowed when touched with the terminals, to a given signal, that the test material was a good conductor of electricity (Platt, 2009). The polyaniline membrane exhibited electrical conductivity attributable to the conjugated π-electron system along its polymer backbone and proton doping, which enables electron delocalization and charge transport. The alternating C=C bonds in the polymer chain facilitate conjugation, forming pathways for electron mobility and thereby imparting conducting properties. The FTIR spectroscopy was employed

to confirm the presence of characteristic polyaniline functional groups, including the quinonoid and benzenoid bands, which verified successful polymer formation. In addition to conductivity measurements, the membrane was examined visually for homogeneity and adhesion to the support matrix, and its structural integrity was evaluated through swelling stability in aqueous media. While FTIR confirmed the chemical structure, future work may incorporate complementary techniques such as XRD, SEM, TEM, UV-Vis, or Raman spectroscopy to fully confirm morphology and crystallinity of the membrane.

4.3 Characterization of the photo active material

The doping of titanium dioxide with iron (III) nitrate was to facilitate the degradation process to be done under ordinary day light conditions. This is due to the band gap of the photo active material being lowered to absorption band in the visible spectrum (Lee *et al.,* 2012). The prepared electrode was therefore able to facilitate advanced oxidation processes as a heterogeneous oxidant of organic pollutants in wastewater. Therefore, it is an effective agent for the degradation of organic pollutants that exist in water.

The doping was confirmed by studying the sample using UV-Vis together with an assembly of integrating spheres to analyze the total diffuse transmittance and diffuse reflectance. The results of the photoactive material before and after doping are given in figure 4.2.

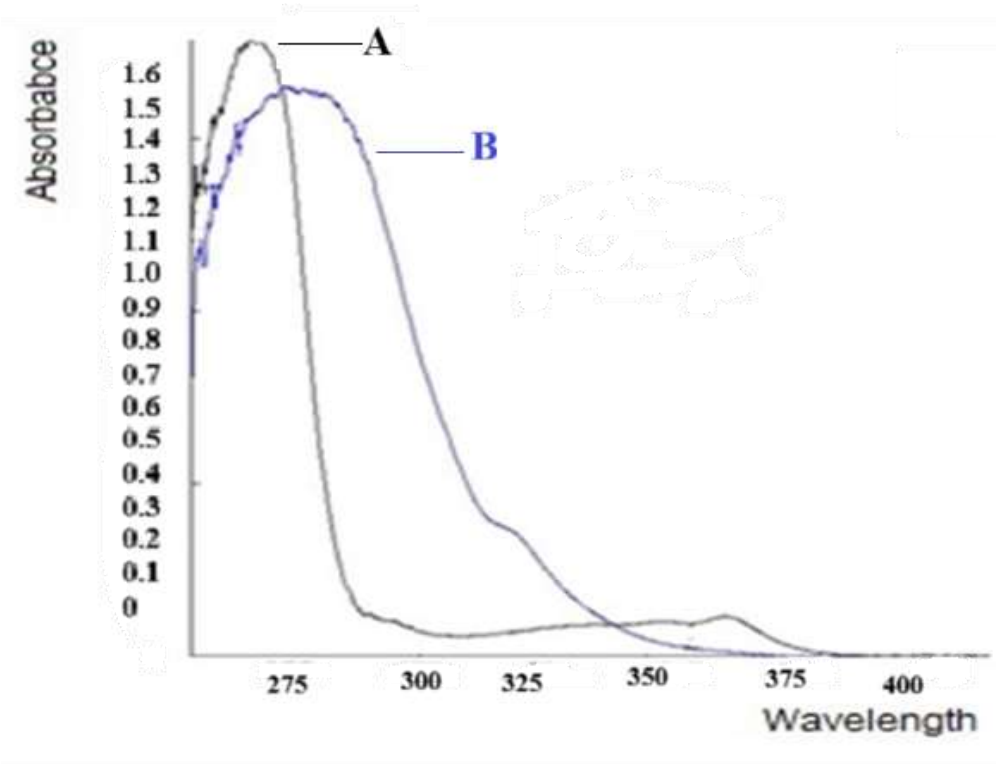

Figure 4.2: The UV-Vis spectra of A undoped and B Fe-doped TiO_2 respectively

The results indicate a variation of photo activity from the UV spectrum to the visible spectrum after doping. It is apparent that doping by pure TiO_2 material (curve A) starts at 250 nm (UV region) with maximum activation at 275 nm and substantially dropping at around 290 nm while the Fe (III)-doped TiO_2 material showed that the absorption starts at 250 nm with the maximum activation occurring at 290 nm. The peak absorption wavelength for the two materials were found to be 275 nm and 290 nm respectively which shows a red shift effect on the spectra (Moradi *et al.,* 2018; Wang *et al.,* 2003). The observed red shift indicates that the introduction of Fe ions into the TiO_2 lattice alters its electronic structure. Even though the absorption remains in the UV region, the systematic red-shift trend is the critical indicator of successful modification of the TiO_2 band structure, which is widely recognized as evidence of Fe-doping. Doping with transition metal ions such as Fe^{3+} creates additional localized energy states within the TiO_2 band gap and enhances electronic interactions between the

dopant and the TiO_2 conduction/valence bands. This modification narrows the effective band gap, thereby lowering the excitation energy required to promote electrons from the valence band to the conduction band. As a result, the absorption edge shifts toward longer wavelengths (visible light region), enabling improved utilization of visible radiation (Lee *et al.,* 2012). The red shift therefore reflects enhanced photoactivity under visible light due to new impurity energy levels, reduced recombination of photogenerated charge carriers, and improved electron–hole separation efficiency introduced by Fe doping (Weng, 2014). The electrode was then used in the assembled cell as an anode for the degradation of dissolved organic matter in real wastewater from green leafy vegetables.

4.4 The X-ray diffraction

The results of powder X-ray diffraction studies of prepared photoactive material, which provide information about the crystal structure are presented in figure 4.3.

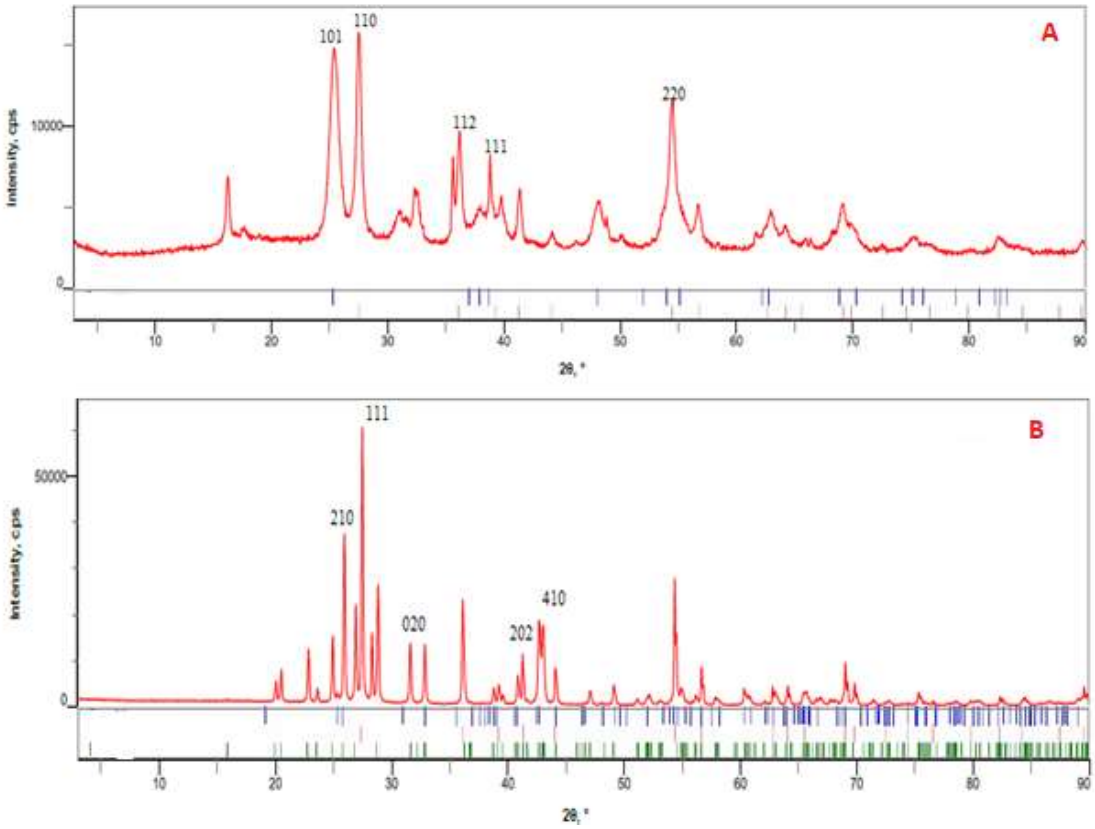

Figure 4.3: The crystalline forms of undoped (A) and Fe-doped (B) titanium dioxide respectively

The crystalline forms of the unmodified titanium dioxide show a combination of both the rutile and the anatase phase, figure 4.3(a). The crystalline form of the iron doped titanium dioxide shows a combination of both the rutile and the anatase phase, however, there was brookite crystal form also obtained as shown in figures 4.3(b). All of them showed a tetragonal structure with space group of 141:141/amd:1, and their unit cell parameters of a = 3.77658 Å b = 3.77658 Å c = 9.41424 Å for TiO_2, a = 3.78572 Å b = 3.78572 Å c = 9.49120 Å for Fe-TiO_2. In general, the lattice parameters increased due to the effect of the metal ions within the structure of the titanium dioxide. As a result, there was an overall increase in the lattice volume from 134.271 Å for TiO_2 to 135.025 Å for Fe-TiO_2.

The iron doping of titanium dioxide is influenced by the charge neutrality that require a decrease in level of oxygen valences and /or formation of interstitial of higher valency. Cationic doping is a p-type of doping where cations are used to cause defects. Cations of bigger radii and higher valency (greater than 4) are known to promote phase transitions. This is because they substitute for Ti^{4+} ions on the crystal lattice, giving rise to destruction of existing large and rigid oxygen sub-lattice vacancies which determine the structural stability, and results to the formation of gaps similar or lower valences enabling the capacity of reorganizing chemical bonds (Sarkar & Khan, 2019). The incorporation of Fe^{3+} cations into vacant Ti^{4+} positions in TiO_2 was possible due to substitution of the similar ionic radius of Ti^{4+} and Fe^{3+} measuring approximately 0.605 Å, , and 0.61 Å, respectively (De Yoreo, 2020).

The XRD results revealed presence of very distinct peaks at specific 2θ values. They corresponded to (110), (111), (020), (121), (400), (202), and (410) crystallographic planes in the Fe-TiO_2. The observed signals were at 2θ values of 25.3, 25.9, 32.8, 38.7, 39.1, 40.8, and 42.6 degrees, respectively. That indicates that the dominant phases found in the doped titanium dioxide are anatase, rutile and brookite. Despite the fact that the particle sizes of the modified samples were found to be within the nano-range, the modification contributed to an increase in particle sizes. That increase was confirmed using the Debye Scherrer's equation 4.1. The TiO_2 particles exhibited sizes ranging from 9.2 nm to 30.0 nm, while the Fe-TiO_2 particles displayed sizes ranging from 43.2 nm to 97.4 nm.

$$D = \frac{K\lambda}{\beta \cos\theta} \qquad (4.1)$$

Where D is the particle size, K is the Scherrer constant, λ is wavelength of the X-ray beam used, β is the Full width at half maximum (FWHM) of the peak and θ is the Bragg angle.

4.5 Scanning electron microscopy-Energy dispersive X-ray (SEM-EDX) analysis

The morphology and the elemental compositions were analyzed using SEM-EDX. The morphology of Fe-TiO_2 particles showed irregular shapes with some surface charge. The elemental composition of the material was analyzed using EDX spectroscopy. It indicated the presence of Ti, O and Fe atoms with weight percentage of 53.0 %, 31.45 % and 14.57 % respectively. The SEM micrographs and the energy dispersive X-ray and composition of the Fe-doped titanium dioxide are shown in figure 4.4 and 4.5 respectively.

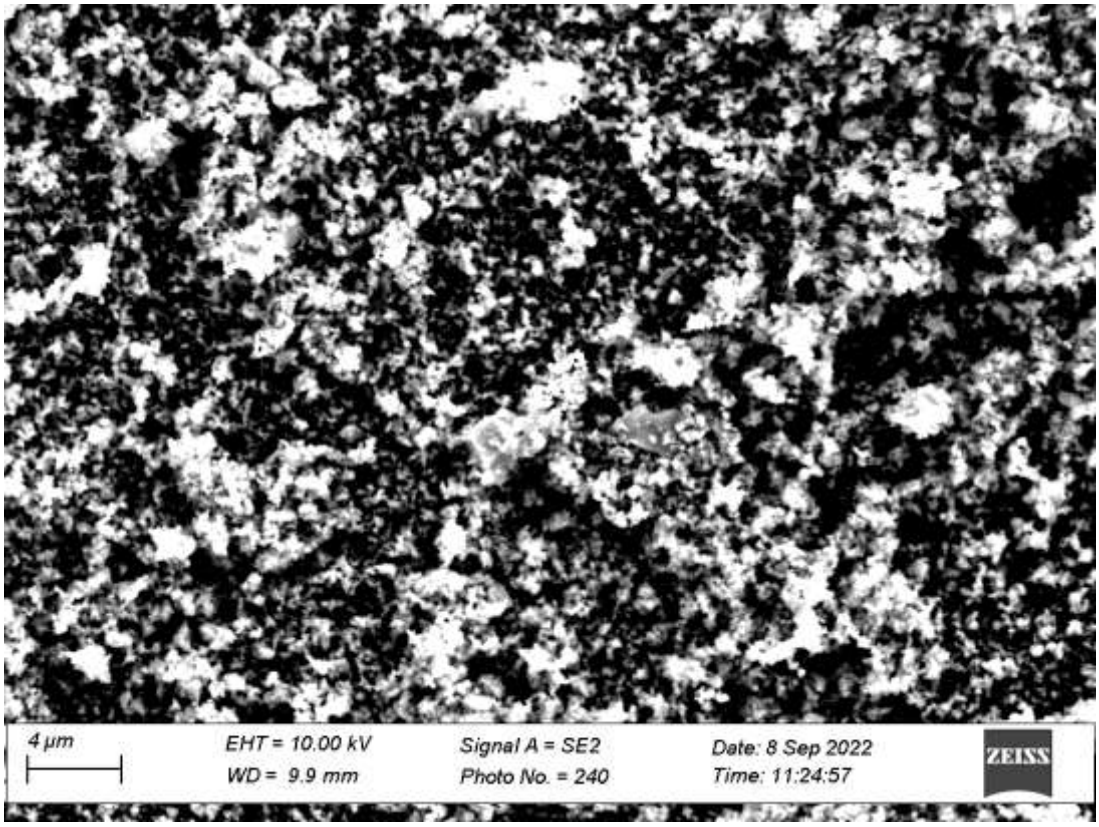

Figure 4.4: The SEM micrograph of the Fe-doped titanium dioxide

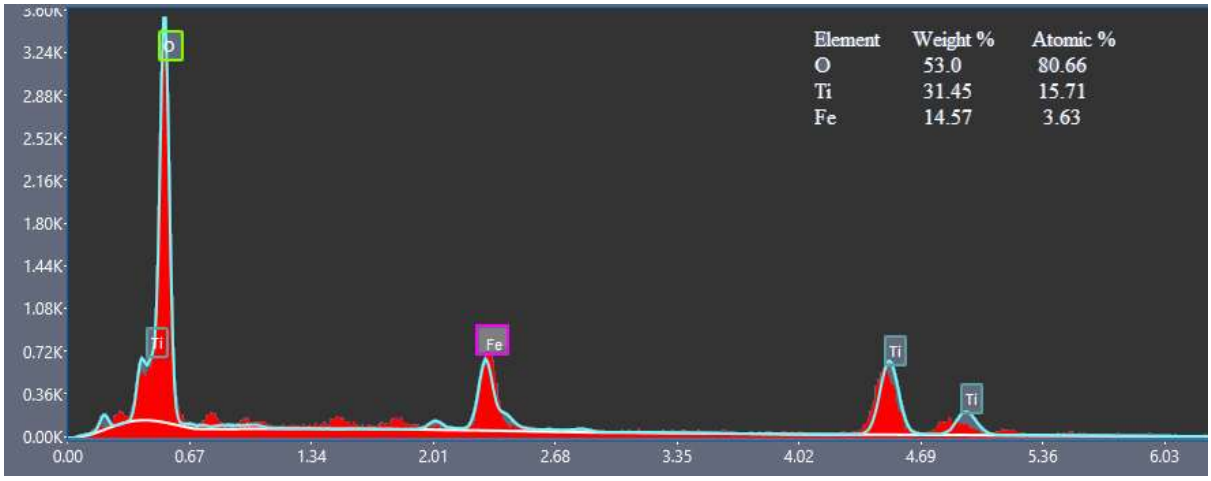

Figure 4.5: The Energy dispersive X-ray and composition of the Fe-doped titanium dioxide

4.6 Potentiometric characterization of the dimensionally stable anode

The modified electrode used in this study served as the dimensionally stable anode and consisted of a graphite rod coated with iron (III)-doped titanium dioxide. Potentiometric and voltametric characterization was performed using a Basi Epsilon analyzer under both dark

and natural light illumination to assess the electrochemical and photo-electrochemical behavior of the electrode. Two experimental conditions were evaluated. In the first setup, the modified electrode acted as the working electrode, the silver/silver chloride (Ag/AgCl) electrode served as the reference electrode, and a platinum electrode functioned as the counter electrode. The Ag/AgCl electrode provided a stable reference potential for accurate measurement of electrode reactions, while the platinum counter electrode completed the electrical circuit and balanced current flow during measurements. In the second setup, the unmodified graphite electrode was used as the working electrode, while the reference and counter electrodes remained the same, enabling comparison of modified versus unmodified electrode performance. Experiments were conducted within a potential window of –0.3 to –0.9 V at a scan rate of 100 mV s^{-1}. Cyclic voltammograms were obtained for domestic wastewater samples dispersed in 0.1 M KCl, and the results presented below correspond to measurements acquired under illuminated conditions using the unmodified electrode as presented in figure 4.6.

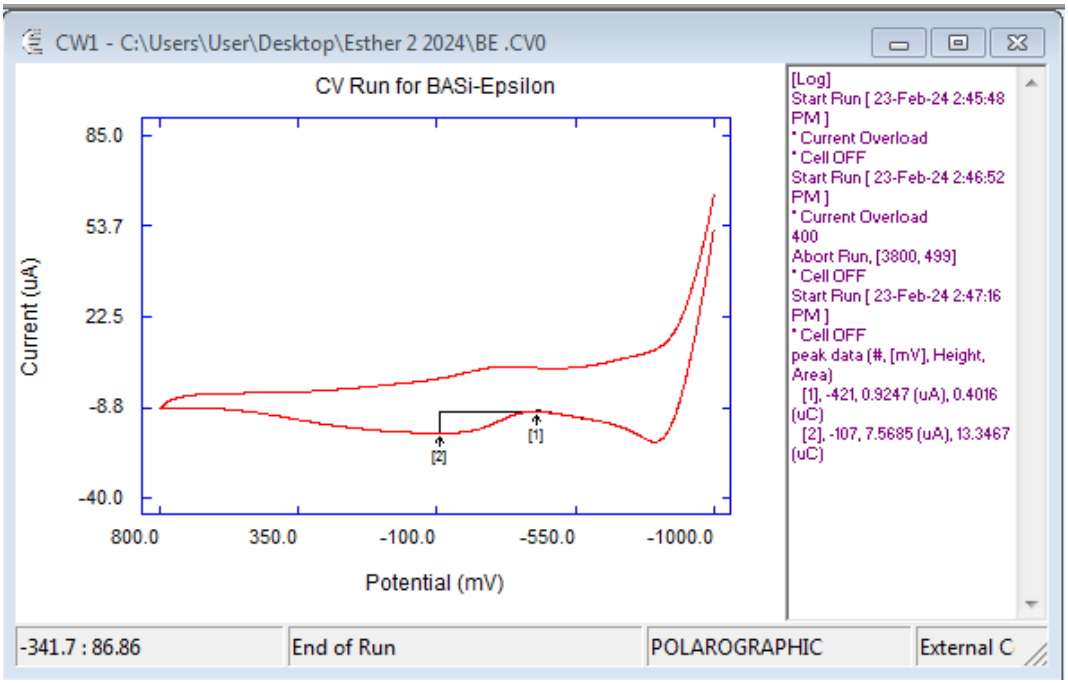

Figure 4.6: The Voltammogram of unmodified graphite electrode vs Ag/AgCl using 0.1M KCl as the electrolyte on potential range -0.3V to -0.9V in dark environment

The results show that neither an oxidation nor a reduction peak was observed within the applied potential range. The experiment was repeated under a dark environment and the results obtained were not any different. These findings indicate that there is neither generated nor existing electro active species in the solution. Therefore, no reduction or oxidation has taken place in the electrochemical cell as the cell is not exposed to radiation (García-Espinoza *et al.,* 2021).

In another experiment, a cyclic voltammogram using iron-doped titanium dioxide coated graphite electrode which is the DSA as a working electrode vs Ag/AgCl was acquired in a dark environment. The set parameters were scan rate of 100 mV/s in 2.0g/L while the domestic wastewater sample was dispersed in 0.1 M KCl with the cell continuously being stirred by bubbling in white spot nitrogen gas. The results obtained were as shown in figure 4.7.

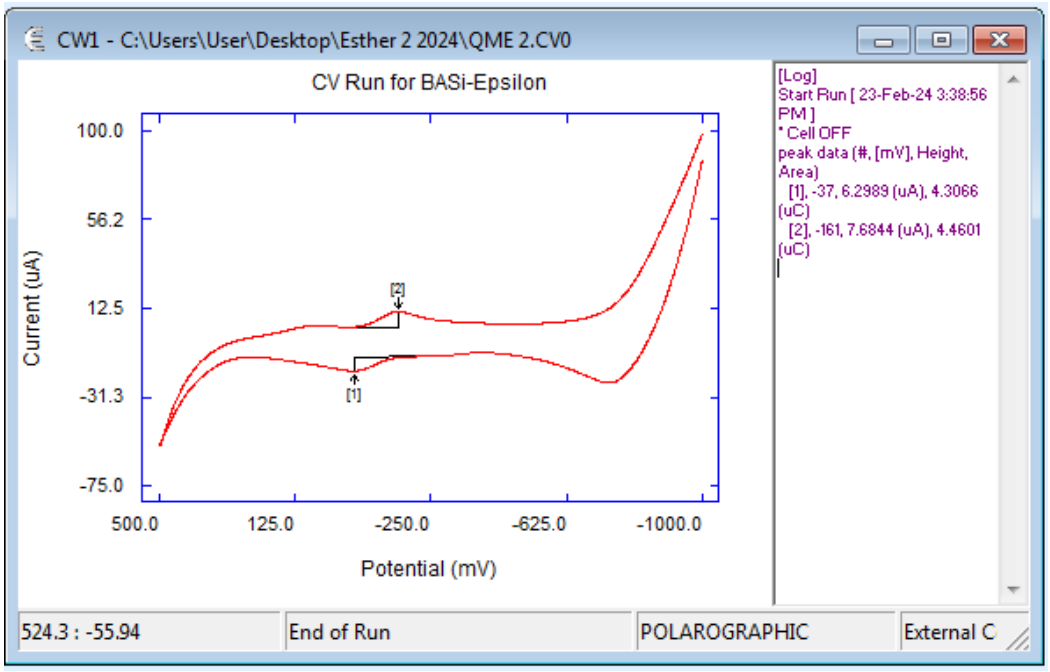

Figure 4.7: The Cyclic voltamogram using iron-doped titanium dioxide graphite electrode as a working electrode vs Ag/AgCl without illumination, scan rate of 100 mV/s in 2.0g/L domestic wastewater dispersed in 0.1 M KCl

The results show a small peak potential of -161.8 mV with a corresponding current of 7.68 µA (anodic) with one cathodic peak at peak potential -37.6 mV and a current of 6.29 µA obtained when the instrument is set at very high sensitivity showing that the generated electroactive species are extremely low.

Another experiment was carried out when the analytical cell was illuminated using natural light under the similar experimental conditions. The results obtained were as presented in figure 4.8.

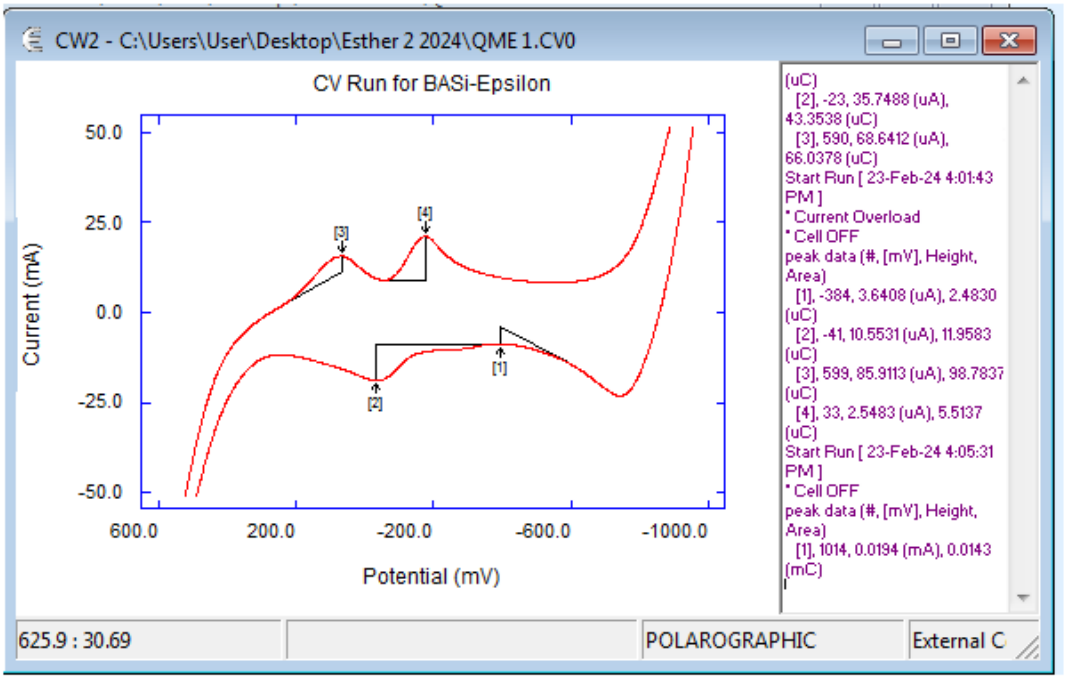

Figure 4.8: Cyclic voltamogram using iron-doped titanium dioxide graphite electrode as a working electrode vs Ag/AgCl illuminated using UV light (254 nm), scan rate of 100 mV/s in 2.0g/L domestic wastewater dispersed in 0.1 M KCl

The results show the presence of two peaks 3 and 4 within the cathodic sweep. This is attributed to the presence of two electro active species that lost some election(s) from the overall charge to some species in the solution which are related to the availability of irradiation. The emergence of peaks could be due to the generation of electro oxidative species due to photo oxidation on the surface of the dimensionally coated electrode (Ruzgys *et al.*, 2019). The peaks 1 and 2 in the anodic sweep confirm the presence of oxidizable species in the solution. This observation of the two peaks is attributed to the fact that dissolved vegetative matter from plants can be divided in two groups as with reference to (Nawaz *et al.*, 2006). Within the same region, there is a reduction (negative potential scan) peak indicating that only one oxidation product is reversible generating anodic peak in the negative scan. These results are similar to an observation by (Elmas *et al.,* 2019; Yadav *et al.,* 2021). The results from this analysis show that the modified graphite coated electrode is sensitive to light

generating strong oxidizing species. This enables *in-situ* oxidation by free hydroxyl radicle like mechanism (Ghasemi *et al.,* 2020). These radicals result into organic radical formation, and electron transfer forming highly reactive species, (H_2O_2 and superoxide $O_2^{\cdot}$) that mineralize the organic molecules (Wang *et al.,* 2021). The presence of these reactive species can be confirmed through indirect probing techniques such as scavenger studies, electrochemical signals associated with radical formation, or spectroscopic detection of intermediate oxidation products. The electrode is then found suitable for in-situ oxidation of domestic wastewater.

Another electrochemical method for the treatment of domestic wastewater at a point of use was investigated. This was by use of platinum electrode as an anode for the generation of strong oxidizing species on its surface. A platinum electrode whose dimensions were 0.45 mm diameter and 7 cm height were used as an anode with bubbling air on its surface. The potential of the cell was registered as 1.24 V when organic content in starch solution was oxidized. This was achieved by the generation of strong oxidizing species on a platinum electrode surface because the platinum surface plays an important role in Pt surface oxide coverage and Oxygen Reduction Reaction (ORR) kinetics (Kongkanand *et al.,* 2023).This result to an oxygen reduction reaction that takes place as shown in the equations 4.2-4.4.

$$O_2 + 4H^+ + 4e^- \rightarrow 2H_2O_2 \quad E^0 = 0.680\,V \tag{4.2}$$

$$2H_2O_2 + 2H^+ + 2e^- \rightarrow 4H_2O \;\; E^0 = 1.776\,V \tag{4.3}$$

The overall equation is as shown below

$$2O_2 + 4H^+ + 4e^- \rightarrow 2H_2O_2 \quad E^0 = 1.240V \tag{4.4}$$

In that experiment, the oxidizing species that reacted with the DOM are as shown in equation 4.5.

$$2H_2O_2 + RCH_2OH + ne^- \rightarrow 2H_2O + CO_2 \tag{4.5}$$

Where R is the carbon tail in the starch molecule chain. That generation of oxidizing species is then found suitable for in-situ oxidation of domestic wastewater. The platinum wire is thus used in a separate experiment as an electrode suitable for *in-situ* oxidation of domestic wastewater.

4.7 Degradation of starch solution

To study the degradation of the model wastewater (starch solution), the anodic chamber of the cell was circulated with a prepared starch solution. The reactor vessel, where a chemical process was intended to occur, aimed to transform domestic wastewater into a desired product namely, clarified water suitable for domestic use. The reactor was designed to achieve this expected product within a reasonable time frame.

During the experiment, the potential across the cell's terminals (reactor vessel) was monitored using a digital multimeter while monitoring the potential after every 10-minute intervals over a two-hour period. The two-hour reaction period was selected based on preliminary trials and literature guidelines demonstrating that significant electro-oxidation activity and observable starch degradation occur within this duration, with minimal additional benefit beyond two hours. This ensured that the reaction captured the key oxidation behavior without unnecessary extension.

Electric potential, defined as the work required to move a unit charge in an electric field, was monitored across the cell to evaluate the electrochemical driving force responsible for forming oxidizing species. Variations in potential over time reflected the progression of electron transfer reactions and consequent degradation of organic contaminants in the model

wastewater. The initial test samples were distilled water (blanks) and the domestic waste water and the results obtained were as shown figure 4.9.

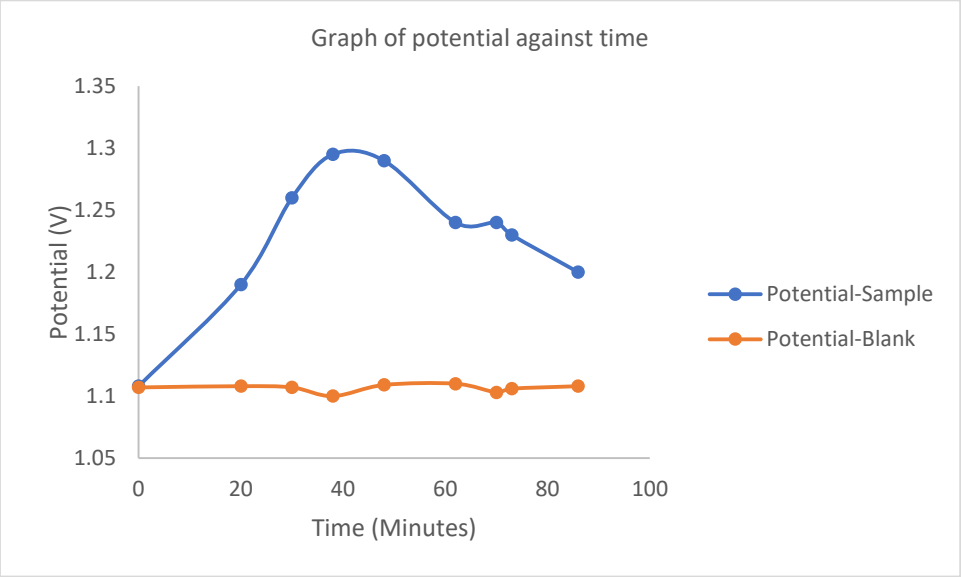

Figure 4.9: Voltage values against time for the degradation of starch solution (sample) and distilled water (blank)

The results show that the oxidation reaction caused the potential of the cell to increase exponentially with the voltage rising to about 1.24 V in the initial 45 minutes. The potential then decreased gradually with time with depletion of the species undergoing oxidation reaction. This observation demonstrates that there is a relationship between electrical potential, as a measurable and quantitative phenomenon, with the electrical potential as an outcome of the chemical change. Electric potential is the amount of driving force needed to move a unit charge from a reference point to a specific point against an electric field.

The first Faraday's laws states that the amount of chemical change produced by migration of electrons at an electrode-electrolyte boundary is proportional to the quantity of electricity used (Emeji *et al.,* 2020). This implies that the amount of substance undergoing an electrochemical reaction (reduction or oxidation) at the electrode-electrolyte interface is

directly proportional to the amount of electricity (charge) that passes through the electrode and electrolyte as according to Faraday's first law as expressed in equation 4.6.

$$\Delta n \propto Q \Rightarrow \Delta n = kQ = \frac{Q}{zF} \tag{4.6}$$

Where

Δn =Change in the number of moles of substance undergoing an electrochemical reaction

z = number of electrons involved

Q = Electric charge

k =constant

F =Charge per mole-Faraday's number

The equation shows that the variation of concentration of the species is proportional to variation in potential. This justifies the variation of analytical parameters being carried out spectro-photometrically which is based on the Beer-Lambert law. As the concentration varies, the driving force (potential) also varies.

According to Beer-lamberts law, the absorbance of a solution is directly proportional to the concentration of the absorbing material present in the solution and path length (Mayerhöfer *et al.,* 2020). By monitoring the changing concentration with time, it indicates the simultaneous change in potential. The analysis was carried out by drawing using a pipette the starch sample solutions (2 mL) from the anodic chamber at regular time intervals of 10 minutes for a period of one hour. To each of the solutions, iodine solution (0.5 mL) was added to form a coloured iodine starch complex which was then analyzed using UV-Vis with the wave band range of 200 nm to 600 nm (Li *et al.,* 2011). The results obtained after the UV–Vis analysis are as presented in figure 4.10.

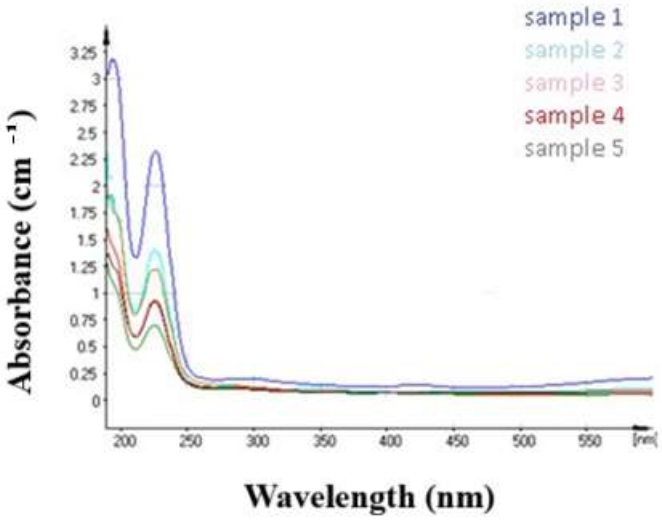

Figure 4.10: UV-Vis spectra for monitoring the degradation process of starch using the assembled cell with the sample marked 1 as the initial sample, while sample marked 5, sample that was taken after an hour (time interval of 10 minutes)

Figure 4.11 show two peaks for absorption maxima (λ_{max}) for the organic matter to be 221 nm and 230 nm. The results obtained in the overlay spectra show a decrease in absorbance with increase in oxidation time as shown by the spectra 1 to 5. The decrease in concentration with time is similar to the observations of potential change observed in figure 4.10 where potential decreased with time due to the degradation of the dissolved organic matter. From the spectra in figure 4.11, the sample marked 1 was the initial sample at the beginning of the redox process, while sample marked 5 is sample that was taken after an hour. The diagram demonstrates compliance with Beer–Lambert's law and also the Nernstian equation through the linear reduction in absorbance with time, indicating proportionality between absorbance and concentration as the starch is oxidized. Although the key analytical region lies within the UV range associated with polysaccharide absorption, the spectrum was recorded from below 200 nm to 550 nm to ensure complete characterization of the sample, validate baseline stability, and detect any intermediate or by-product species formed during electro-oxidation. The observation is similar to that reported by Islam and coworkers (Islam *et al.,* 2019) as they

monitored the degradation of low molecular weight chitosan using UV-Vis spectroscopy. In this study, it is observed that the DOM content decreased as confirmed by the decrease in the absorbance of the water sample.

The absorbance values obtained from the oxidation process were plotted against time, and the results obtained were as presented in figure 4.11.

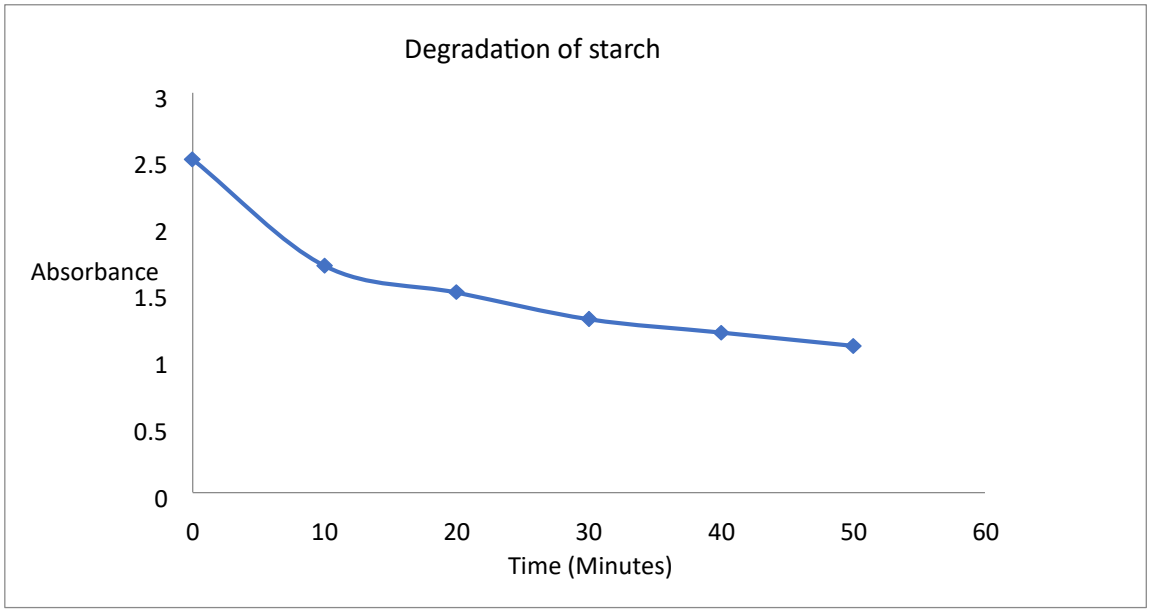

Figure 4.11: A plot of absorbance against time showing degradation of starch

It was observed that the DOM decayed exponentially. The percentage starch removal efficiency was 52% after one hour as determined by equation 4.7.

$$\%\ removal\ at\ time\ t = \frac{A_0 - A_t}{A_0}\ x\ 100 \qquad 4.7$$

where A_0 is the absorbance at t=0 and A_t is the absorbance at sampling time t. The data was analyzed using the first and second-order kinetics to investigate molecularity of the decay (Ho *et al.,* 2000). The first and second-order kinetic equations meant to linearize the relationship between absorbance against time are expressed in equations 4.8 and 4.9 respectively:

$$Abs = kt + C \tag{4.8}$$

$$\frac{1}{Abs} = kt + C \tag{4.9}$$

Where

$|A|$ =Absorbance of radiation

k =Proportionality constant (slope)

C =Intercept

The results obtained were presented in figure 4.12.

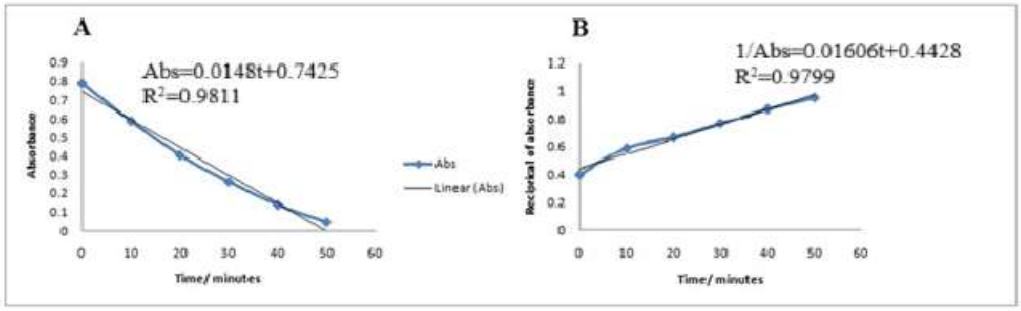

Figure 4.12: Kinetic data for (A) first order and (B) second order kinetics for degradation of starch solution

The figure shows that the linear regression in A, which is for the first order, is higher than the second order kinetics in B. This suggests that the decay of organic matter in wastewater followed first-order kinetics which is unimolecular degradation with a constant of 0.0148. Other species in the wastewater did not interfere with the electro-oxidation process of the dissolved carbon, confirming that degradation reaction was a time-dependent process. This means that as the redox process continued in the cell, there was depletion of the dissolved carbon material hence reducing the concentration of the DOM in wastewater. Therefore, the wastewater is purified with time as the redox process progressed.

4.8 Degradation of organic matter in vegetable wastewater

The assembled cell was then used for degradation of the organic matter in domestic wastewater. The organic matter was a heterogeneous class of water-soluble multicomponent of both organic and inorganic nature that are water soluble. The properties of the sample domestic wastewater before and after treatment are recorded in table 4.1.

Table 4.1: Parameters of the domestic wastewater before and after the electro-oxidation process

PARAMETER	***UNITS***	***SAMPLE*** **UNTREATED**	**After 120 minutes**	**After 3600 minutes**
Electrical conductivity, EC	µS/cm	1260	860	750
pH	-	7.3	7.3	7.6
Colour	Pt-Co units	5.0	5.2	4.6
Turbidity	NTU	700	500	210
Total Hardness	mg/l	136	110	96
Total Alkalinity	mg/l	8.5	5.3	4.5
Total dissolved solids, TDS	mg/l	630	430	375
Total Suspended solids, TSS	mg/l	18	8	5
Sulphate	mg/l	560	70	55
Chloride	mg/l	700	375	490
Total phosphorus, TP	mg/l	9.6	5.6	4.4
Total nitrogen, TN	mg/l	16.4	8.6	6.4
Total organic carbon, TOC	mg/l	2.8	2.4	1.6
Volatile suspended solids, VSS	mg/l	1.2	0.0	0.0
Fats, Oil and Grease	mg/l	0.8	0.0	0.0
Chemical oxygen demand, COD	mg/l	120	80	55
Biochemical oxygen demand, BOD	mg/l	40	24	14
Iron	mg/l	5.88	6.54	0.66
Copper	mg/l	3.53	5.10	2.15
Chromium	mg/l	0.52	0.77	0.32
Lead	mg/l	0.04	9.01	0.00
Zinc	mg/l	6.40	6.26	3.41

Due to logistical and instrumentation limitations, each physio-chemical parameter was measured once per sampling point. Therefore, standard deviations are not reported. Future

studies should include replicate sampling to strengthen statistical reliability. The results show a distinct variation of the parameters analyzed. The color of the sample water was analyzed using the Pt-Co method, and it is evident that the removal of species responsible for coloration as the Pt-Co units decreased from 5.2 to 4.6 in the treated wastewater. This is because Platinum-Cobalt colour scale ranges from 0 to 500 with the lowest value at "0" referring to water as white or "distilled and a 500 value on the scale means the water is distinctly yellow (Yang *et al.,* 2020). The degradation of the same domestic wastewater was done by electro-oxidation in the reactor cell designed by this study. It was conducted in a natural-light illuminated setting, and a digital voltmeter was used to track the degradation process and the potential difference between the electrodes of an electrochemical cell was recorded. The recorded results are shown in figure 4.13.

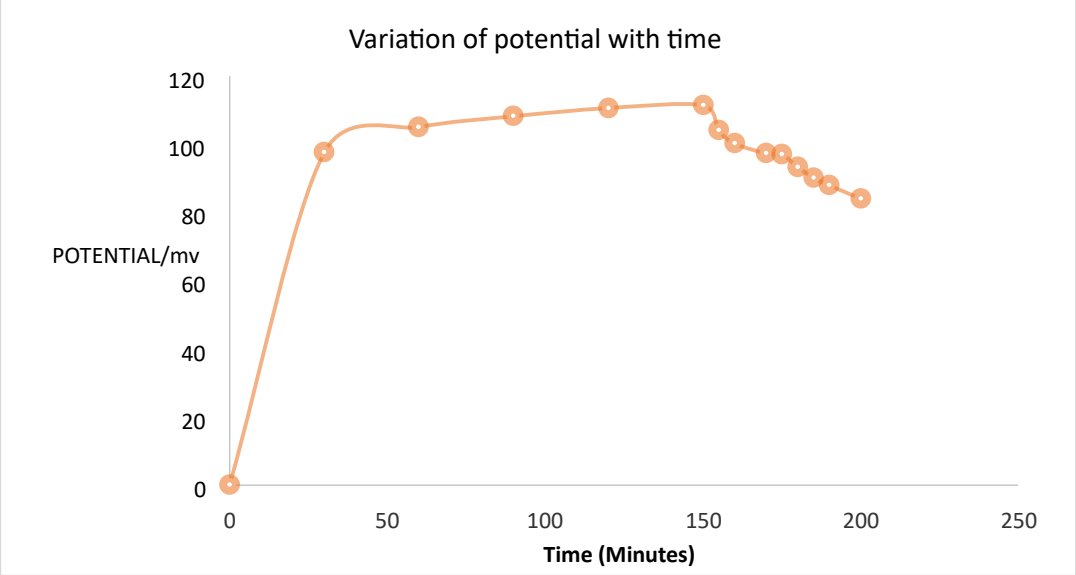

Figure 4.13: The variation of potential difference of the electrochemical cell

The results indicate that the cell registered a high voltage of approximately 105 mV in the first $2^1/_2$ hours of the oxidation process. Thereafter the potential begins to reduce with time at a relatively high rate. This observation is attributed to the reduction in the oxidizable

species due to the redox reaction or anode deactivation. The concentration changes of the species undergoing oxidation are proportional to the adsorption rate and the catalytic reactions taking place at the anode, hence the deactivation of the electrode (Berger *et al.,* 2012; Kumar *et al.,* 2015).

4.9 Cyclic voltammetry (CV) analysis of the degraded wastewater

An attempt to further understand the effect of redox reaction to the inorganic substances in the wastewater was carried out using a potential stat-Basi Epsilon analyzer. The cyclic voltametric method was used to study the electro-oxidation process. Samples of 2 mL samples were drawn from the reactor at half-hour intervals and introduced to the electro-analyzer cell. The measurements were conducted when the samples were put in a potassium nitrate solution (0.1 M) that was then repeatedly stirred by white spot nitrogen gas that was bubbling. The electro-analyzer cell's potential sweep range was fixed between −1.0 and 0.8 V (vs. SCE) with a scanning rate span of 1–100 mV s^{-1}. The experiments were carried out at a room temperature of 25 °C and the results achieved are shown in figure 4.14.

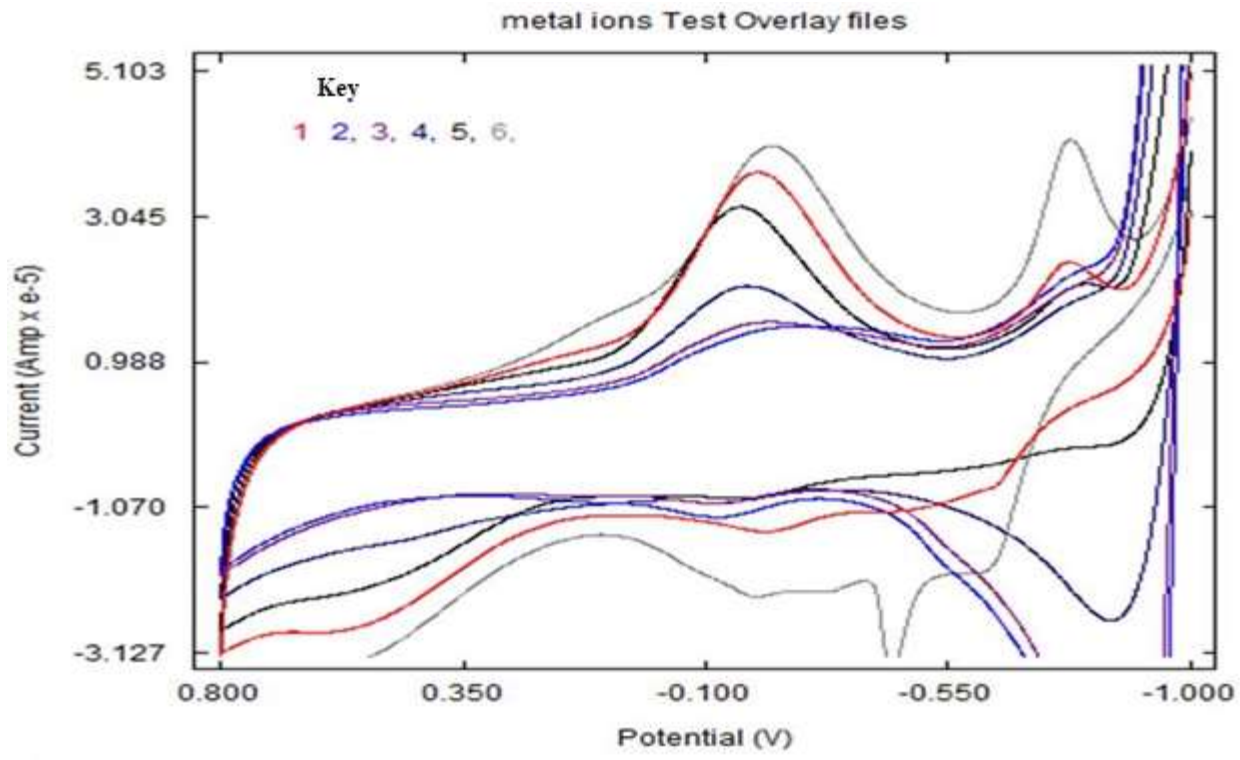

Figure 4.14: Cyclic voltammograms of the degraded wastewater over time during treatment

The figure shows distinct redox responses that evolve with treatment time. The progressive increase in peak current and changes in peak position reflect the release and redox transformation of electroactive species during degradation of dissolved organic matter. Sample 1 (0 min) shows the lowest redox activity, while Sample 6 (end of treatment) exhibits the highest peak currents, consistent with increasing concentration of released inorganic ions over time. This confirms that the electro-oxidation process is time-dependent, and that oxidation of organic matter results in measurable electrochemical changes in solution (Pipi *et al.,* 2013).

A notable peak observed around −0.18 V (vs SCE) is attributed to surface-bound and subsequently released Fe^{3+}/Fe^{2+} transitions. This assignment is consistent with reported studies on iron-containing systems showing similar redox signatures (Toh *et al.,* 2014). The

peak was absent in the initial blank electrolyte and in voltammograms recorded with the unmodified electrode, confirming its origin from the iron-modified electrode and from iron species released during electro-oxidation. These findings therefore indicate that iron associated with the oxidized organic complexes enters solution gradually during treatment. This observation aligns with changes in physicochemical parameters in table 4.1, confirming increased metal ion release and subsequent reduction in dissolved organic matter.

The voltammograms do not exhibit the classical reversible peak patterns typically seen in simple electrochemical systems. Instead, the broad, asymmetric signals and peak shifts arise from interaction between electrochemical oxidation and photocatalytic reactions and evolving matrix composition as contaminants degrade. The cyclic voltammetry analysis demonstrates that electro-oxidation gradually releases electroactive iron species and simultaneously degrades dissolved organic matter in a time-dependent manner. The evolution of peak currents and potential shifts confirms active redox behavior associated with catalyst-mediated oxidation, validating the efficiency of the developed electrode for wastewater purification (Tan *et al.,* 2023).

4.10 Time dependent clarification

4.10.1 Time dependent clarification using a platinum electrode

Over time, the decrease in the reactant concentrations leads to a reduction in reaction rates. To understand this phenomenon, the changes in wastewater clarity were monitored over an extended period. The degradation rate of dissolved organic matter while using a platinum electrode by regularly drawing 5 mL wastewater samples from the anode solution after every 30 minutes for a total duration of three hours. The samples were abbreviated as 1-5, ranging from initial (sample 1) to sample after three hours, (sample 5). These samples were then

analyzed using a UV-Vis spectrophotometer within a wavelength range of 270 nm to 300 nm. This spectroscopy method is known for its ability to identify DOM composition, source, and reactivity (Li & Hur, 2017). The findings are displayed in figure 4.15.

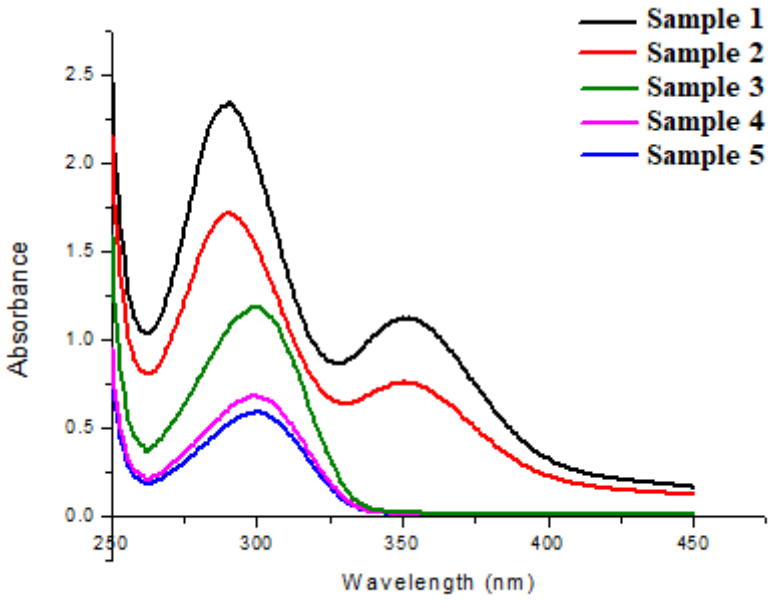

Figure 4.15: The spectra of the degradation of dissolved organic matter with time

The results obtained show a peak of maximum absorption at 300 nm wavelength. This is attributed to the presence of dissolved small molecular organic matter after the oxidation of the complex organic matrix of the green leafy sample wastewater (Lei *et al.,* 2019). It was observed that the concentration of the oxidized products from the complex organic matrix decreased as shown from the initial sample 1 to the sample (6) after three hours, of oxidation time. The optical analysis of transparency of water was monitored with time using a UV-Vis spectrophotometer at 300 nm. The results show that despite the release of free iron into the solution which gave a brown-colored solution confirmed by cyclic voltammetry, the coloration of water was cleared. This implies that all the species dispersed in the water are oxidized and removed from the water. The absorbance data plots are shown in figure 4.16.

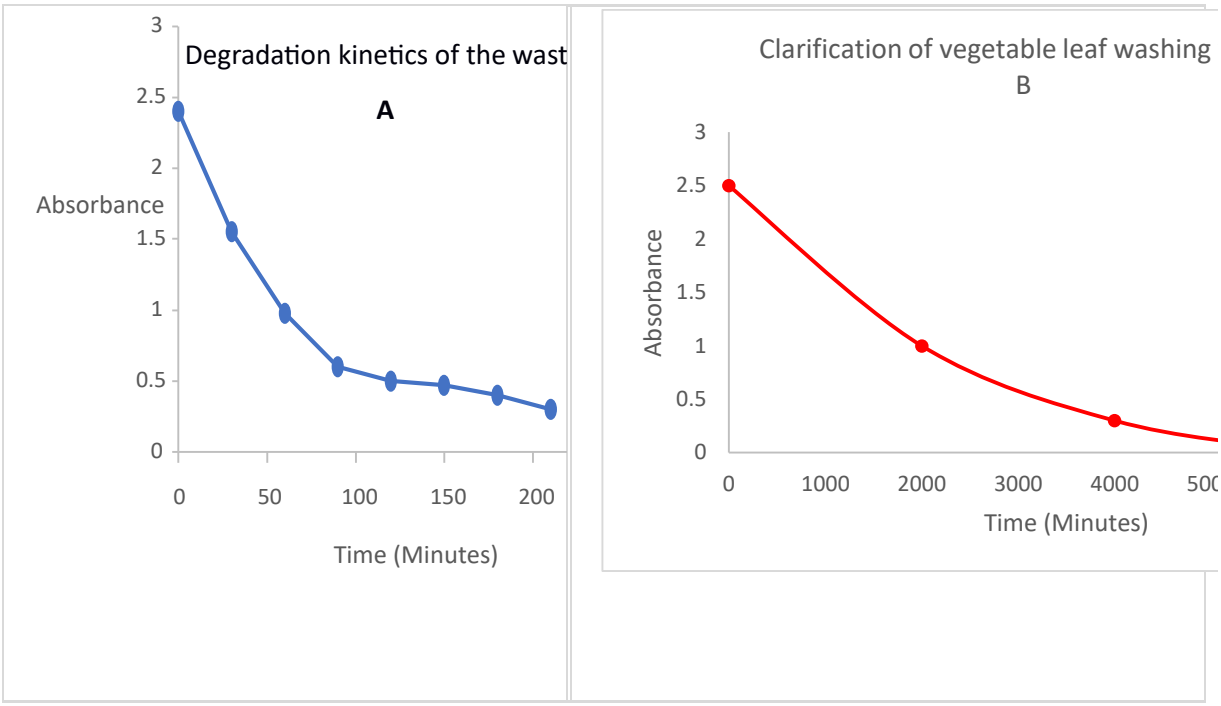

Figure 4.16: Absorbance data plotted against time in (A) and Time dependent clarification of the wastewater in (B)

The results indicated a reduction in absorbance with time, demonstrating that the electrochemical process for the dissolved species (inorganic or organic) that had dispersed in water decayed exponentially with time. This suggests that with continued redox process in the cell, there is a steady depletion of any dissolved matter in the sample wastewater resulting to improved clarity as shown in figure 4.16 B. The data obtained was treated with the first and second order kinetic models represented by equations (4.8) and (4.9). This was to determine the molecularity of the degradation process with a view to establishing the number of species that affect the oxidation process (Woo *et al.*, 2020). The outcomes of the first and second order models were as shown in figure 4.17.

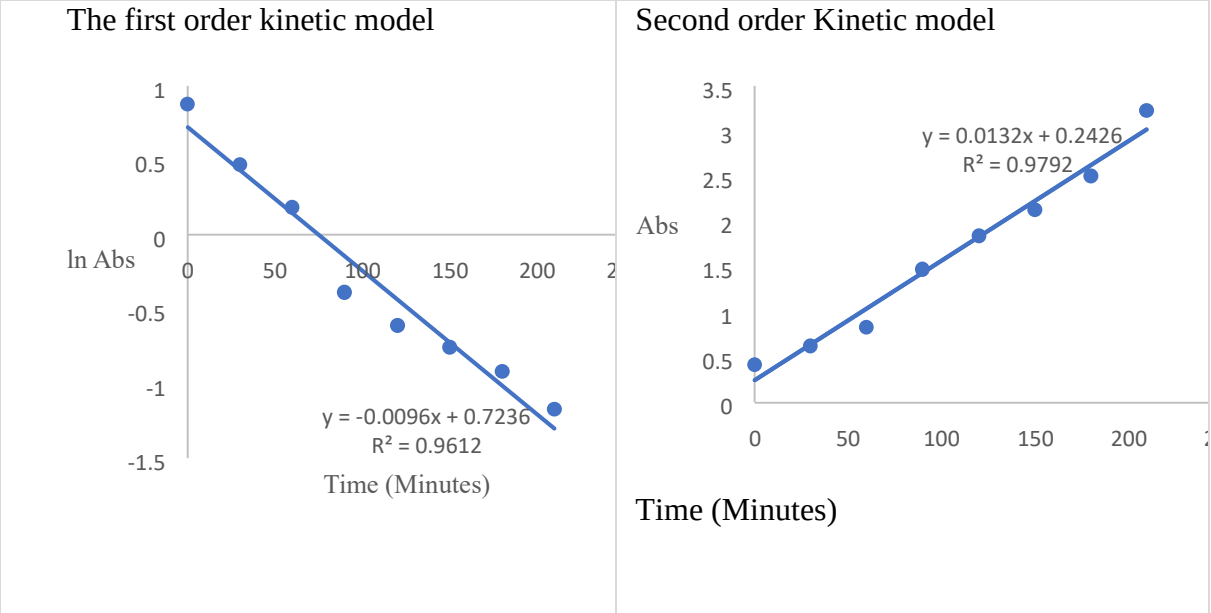

Figure 4.17: First and second order degradation kinetics of the domestic wastewater

The individual plots produced straight lines with a correlation coefficient of $R^2 = 0.9612$ for first order kinetics while it was $R^2 = 0.9792$ for second order kinetics hence proving that the electrochemical process for the degradation of organic substances is bimolecular of second order kinetics. This is the case because there are other species in the water that are electroactive and are electro oxidized alongside the organic matter. This is as shown in the cyclic voltametric analysis which indicated the presence of dissolved iron as evidenced by signals recorded as -0.180 V (Toh *et al.*, 2014). That is one of the other species in the solution affected by the electro-oxidation hence an overall a second order electro-oxidation. The iron (III) ions are oxidized to form an insoluble substance (sludge) that settles at the bottom of the reactor vessel as can be seen in figure 4.9. The degradation process is therefore time-dependent reaction as demonstrated by the increase in clarity of the water with time capable of removing both organic and inorganic pollutants from water.

4.10.2 Time dependent clarification- using the iron (III) doped titanium dioxide coated dimensionally electrode

The degradation rate of dissolved organic matter in the water sample was analyzed and the analyte sampled in a similar manner as in section 4.10.1 while using the iron (III) doped titanium dioxide coated dimensionally electrode. The coating made it possible for the oxidation process to be activated by the visible radiation as reported by Moradi and co-workers (2016). The wavelength of maximum absorption was observed at a wavelength 300 nm similar to the case in above section. This is because the species being analyzed are the same. The degradation kinetics data obtained was as presented in figure 4.18.

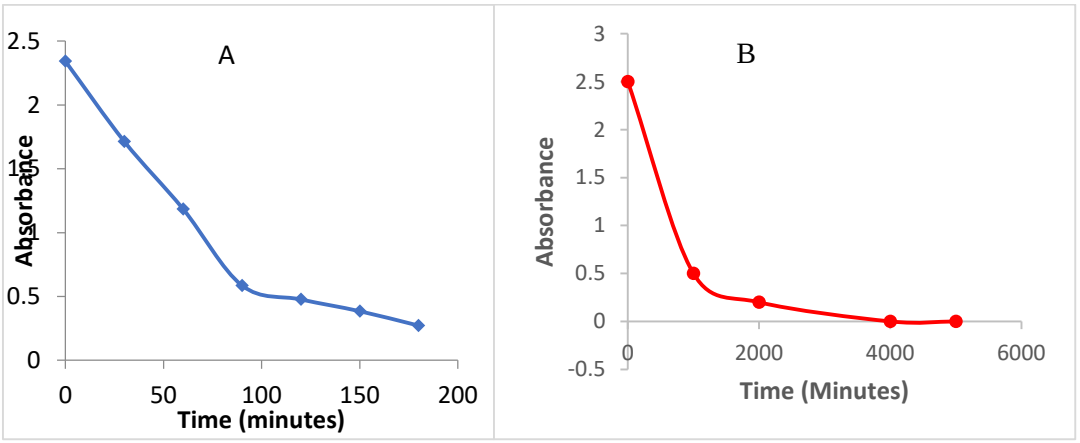

Figure 4.18: Absorbance data plotted against time in (A) and Time dependent clarification of the wastewater in (B)

The results depict a reduction in absorbance with time, suggesting that the electrochemical process cause the dissolved organic matter to decay exponentially. The degradation process is also shown to be a time-dependent reaction signifying that prolonged redox process in the cell leads to a depletion of the dissolved organic matter content in the wastewater as depicted in figure 4.18 B. This explained that by the use the photo-active DSA there is evidence of the formation of reactive species on its surface (García-Espinoza *et al.,* 2021). The data obtained on the degradation using the DSA above was treated with the first and second order kinetic

models expressed in equations (4.8) and (4.9) respectively. The data obtained was as presented in figure 4.19.

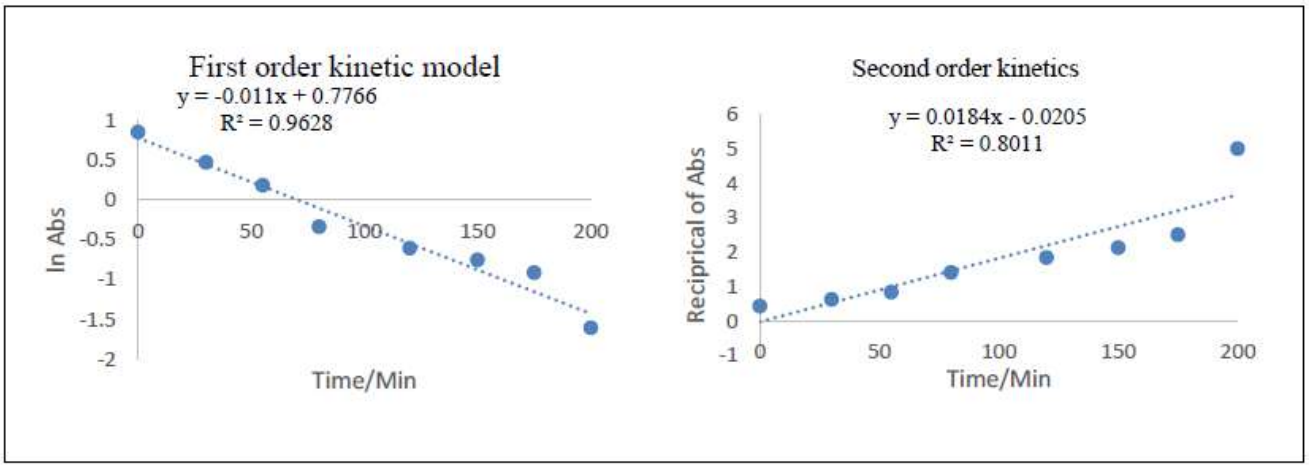

Figure 4.19: First and second order degradation kinetics for the degraded domestic wastewater

Based on the values of co-efficient of correlation values, the degradation prescribed to first order kinetics of unimolecular electro-oxidation. This was to establish the molecularity of the degradation process with a view of the number of species that affect the oxidation process (Woo *et al.,* 2020). The presence of iron (III) had earlier been confirmed in the cyclic voltammetry experiments. However, kinetic studies do not show a second order degradation as was observed while the oxidation took place at the platinum anode oxidation. This was despite the release free unbound iron (III) ions released from the vegetative mater dispersed in water. This could imply that only one specie is available in the electro oxidation process. The observation could be explained by recent studies by Abebe and Ananda (2018) who confirmed that nanosized titania has a number of unique properties. In their study, they reported that titanium dioxide agglomerates with iron oxides to form particulate adsorbents with a large number of adsorptive sites by impregnation method (Abebe & Ananda Murthy, 2018). This is contributed by the fact that titanium dioxide forms different types of metal oxides, and with presence of iron in wastewater oxides of γ-Fe_2O_3, α-Fe_2O_3, and Fe_3O_4 could

have been formed (Porter *et al.,* 2018). The affinity of titanium dioxide to iron ions released from wastewater leads to their agglomeration, which can be confirmed using the SEM-EDX, and XRD analysis of the sample and therefore removal from the solution. This resulted to the generation of oxidizing species which interacted with the dissolved matter lowering the concentration (of the dissolved matter) in the water (Ferroni *et al.,* 2021). The transparency (clarity) of the treated water increased with time and the color change was clearly observable as it happened. The green leafy (parent water sample) colored solution transited from green to a brown evenly dispersed colored solution, and then cleared after 72 hours of continuous oxidation. It should be noted that half of the treatment process was met by the night and there was no solar radiation.

The samples obtained from the above process were simultaneously analyzed for dissolved organic matter using the starch iodine complex method. This is based on the formation of colored starch iodine complexes (Li *et al.,* 2011; Louis & Gabriel, 2014). It was done by addition of iodine a constant amount of iodine to each sample separately and the resulting color variation monitored using UV-Vis spectrophotometer and the results presented in figure 4.20.

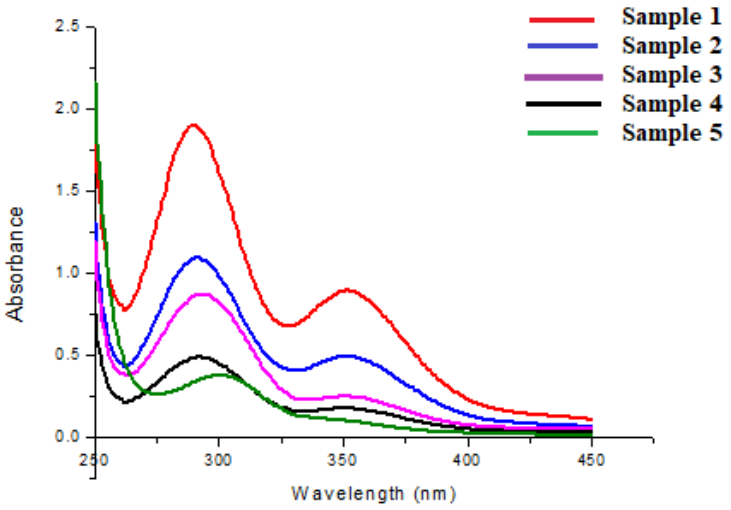

Figure 4.20: The spectra of iodine complex of the dissolved organic matter

The results show peaks between 275-300 nm and between 325-375nm. The maximum absorption of radiation found at 290 nm is attributed to the chromophore $I^- \cdot I^-$ complex (Moulay, 2013; Mwangi *et al.,* 2013). This leads to the suggestion that the oxidation process of the dissolved organic matter in the green leafy vegetable water sample results to smaller molecules of starch which complex with the iodine solution (Hansen *et al.,* 2016). The signal profile confirmed that the samples that had undergone oxidation as evidenced by their sizes. The shortest treatment time had a high absorbance value while the highest treatment time showed the lowest absorbance value. The relation between the clarity and the treatment time is directly proportional. This indicates that the more the oxidation time, the higher the degradation of starch compounds by the oxidation process of the organic matter in the green leafy solution.

During the treatment process, the color of the sample water transited from light green/yellow to dark brown solution which is likely due to oxidation of the organic starch material to carbon dioxide and water resulting to the release of iodine from the starch-iodine complex. This is similar to what was reported by Redel and co-workers (2009) as they studied a starch-

iodine model in inorganic–organic hybrid compounds. They observed that the deep blue color of starch– iodine also disappears when air is bubbled through its colloidal solutions due to the oxidation of the iodate ion to iodine (Redel *et al.,* 2009).

CHAPTER FIVE

CONCLUSIONS AND RECOMMENDATIONS

5.1 Conclusions

This study aimed to develop a sustainable electrochemical cell for the oxidation of organic matter in domestic wastewater, adapted from a microbial fuel cell concept. The study objectives were successfully achieved as outlined below:

To prepare and characterize an inert conducting polymer synthesized from aniline for use as a proton exchange membrane in the cell. A conducting polymer synthesized from aniline was successfully prepared and incorporated into a hydrogel matrix before being cast on a sintered glass frit to form a proton exchange membrane (PEM). The membrane was reinforced with calcium silicate to improve mechanical strength. FTIR analysis confirmed the presence of functional groups characteristic of polyaniline, verifying successful synthesis, while conductivity measurements showed good proton transport properties suitable for application in an electrochemical cell.

To prepare and characterize a photoactive material for coating on a dimensionally stable anode (DSA) of the cell. A Fe(III)-doped titanium dioxide photocatalyst was prepared and used to dip-coat a graphite anode to render it photoactive. UV–Vis spectroscopy revealed a red-shift in the absorption spectrum, confirming enhanced sunlight absorption due to Fe doping. SEM-EDX confirmed the incorporation of iron ions within the TiO_2 matrix, and XRD analysis verified the crystalline phase of the material, indicating successful modification.

To characterize the coated dimensionally stable anode electrode. Electrochemical characterization using cyclic voltammetry demonstrated improved redox activity and electron transfer properties of the Fe(III)-doped TiO_2-coated electrode compared to the unmodified one. The electrode exhibited enhanced current response under natural light illumination, confirming its effectiveness as a photoactive DSA for oxidation reactions.

To determine the degradation kinetics of dispersed organic species in model wastewater solutions using the assembled electrochemical cell with a platinum anode electrode.

An electrochemical cell with two glass compartments separated by the synthesized PEM was successfully assembled. The platinum electrode system achieved a peak potential of approximately 1.24 V within 40 minutes, maintaining a stable voltage of 1.2 V throughout the oxidation process. The degradation of dissolved organic matter (DOM) in the model starch solution followed first-order kinetics, indicating unimolecular electro-oxidation triggered by reactive oxygen species generated on the platinum surface.

To determine the degradation kinetics of dispersed organic species in model wastewater solutions using the assembled electrochemical cell with a dimensionally stable anode.

The Fe(III)-doped TiO_2-coated graphite electrode demonstrated effective oxidation of organic species in a real wastewater sample derived from green leafy vegetable washings. UV–Vis and potential measurements indicated a progressive reduction in DOM concentration over time, with a maximum voltage of 105 mV recorded within 2.5 hours. The DSA electrode, however, exhibited deactivation after approximately 12 hours, whereas the platinum anode remained active for up to 48 hours. The system purified 4.5 g/L of green leafy extract within 72 hours, and the degradation process followed first-order kinetics, showing independence from intermediates or secondary species.

These findings confirm that the developed electrochemical cell offers a cost-effective, sustainable, and environmentally friendly approach for point-of-use wastewater purification, contributing toward the realization of sustainable development goal 6, 9, 12 and 13.

5.2 Recommendations

i. The assembled electrochemical cell can be effectively used for the electro-oxidation of dissolved organic matter in wastewater.
ii. It is suitable for small-scale or point-of-use domestic wastewater remediation.
iii. This approach offers a promising method to reduce water pollution and mitigate environmental contamination.

5.2.1 Recommendation for future work

i. Explore alternative conducting polymers and photoactive electrodes to enhance performance and durability.
ii. Conduct studies to reduce deactivation of the DSA electrode, improving its operational efficiency.
iii. Investigate the potential for electricity generation during wastewater treatment, similar to microbial fuel cells.
iv. Develop hybrid advanced oxidation processes by combining two or more treatment methods for improved wastewater purification.
v. Optimize other components and operational parameters of the electrochemical cell to enhance overall efficiency.

REFERENCES

Abebe, B., & Ananda Murthy, H. (2018). Synthesis and characterization of Ti-Fe oxide nanomaterials for lead removal. *Journal of Nanomaterials*, *2018*, 1-10.

Aelterman, P., Rabaey, K., Clauwaert, P., & Verstraete, W. (2006). Microbial fuel cells for wastewater treatment. *Water Science and Technology*, *54*(8), 9-15.

Al-Mamun, M., Kader, S., Islam, M., & Khan, M. (2019). Photocatalytic activity improvement and application of UV-TiO_2 photocatalysis in textile wastewater treatment: A review. *Journal of Environmental Chemical Engineering*, *7*(5), 103-248.

Amer, I., & Young, D. A. (2013). Chemically oxidative polymerization of aromatic diamines: The first use of aluminium-triflate as a co-catalyst. *Polymer*, *54*(2), 505-512.

Amorós-Pérez, A., Cano-Casanova, L., Castillo-Deltell, A., Lillo-Ródenas, M. Á., & Román-Martínez, M. d. C. (2018). TiO_2 modification with transition metallic species (Cr, Co, Ni, and Cu) for photocatalytic abatement of acetic acid in liquid phase and propene in gas phase. *Materials*, *12*(1), 40.

Bartolomeu, M., Neves, M. G. P. M. S., Faustino, M. A. F., & Almeida, A. (2018). Wastewater chemical contaminants: Remediation by advanced oxidation processes. *Photochemical & Photobiological Sciences, 17*(11), 1573–1598. https://doi.org/10.1039/C8PP00249E

Bekyarova, E., Sarkar, S., Wang, F., Itkis, M. E., Kalinina, I., Tian, X., & Haddon, R. C. (2013). Effect of covalent chemistry on the electronic structure and properties of carbon nanotubes and graphene. *Accounts of Chemical Research*, *46*(1), 65-76.

Berger, T., Monllor-Satoca, D., Jankulovska, M., Lana-Villarreal, T., & Gomez, R. (2012). The electrochemistry of nanostructured titanium dioxide electrodes. *ChemPhysChem*, *13*(12), 2824-2875.

Bhateria, R., & Jain, D. (2016). Water quality assessment of lake water: a review. *Sustainable Water Resources Management*, *2*, 161-173.

Bienkowski, K. (2006). *Polyaniline and its derivatives doped with Lewis acids-synthesis and spectroscopic properites* (Doctoral dissertation, Université Joseph-Fourier-Grenoble I; Warsaw University of Technology).

Boddula, R., & Srinivasan, P. (2014). Emeraldine Base form of polyaniline nanofibers as new, economical, green, and efficient catalyst for synthesis of Z-Aldoximes. *Journal of Catalysts*, *2014(1), 515428.*

Bond, D. R., Holmes, D. E., Tender, L. M., & Lovley, D. R. (2002). Electrode-reducing microorganisms that harvest energy from marine sediments. *Science*, *295*(5554), 483-485.

Brini, E., Fennell, C. J., Fernandez-Serra, M., Hribar-Lee, B., Luksic, M., & Dill, K. A. (2017). How water's properties are encoded in its molecular structure and energies. *Chemical reviews*, *117*(19), 12385-12414.

Butt, M. S., & Sultan, M. T. (2018). Nutritional Profile of Vegetables and Its Significance in Human Health. *Handbook of Vegetables and Vegetable processing*, pp157-180.

Carbonari, G., Maroni, F., Pasqualini, M., Tossici, R., & Nobili, F. (2017). Preparation and Electrochemical Characterization of High-Stability MnO Anodes for Li-Ion Batteries. *Electrochimica Acta*, *247*, 392-399.

Cano-Castillo, U. (2013). Hydrogen and fuel cells: potential elements in the energy transition scenario. *Revista Mexicana de Física*, *59*(2), 85-92.

Chen, G., Chen, X., & Yue, P. L. (2019). Separation processes and purification technology for wastewater treatment. *Separation and Purification Technology, 16*(1), 15–23.

Cheng, Y. (2015). Advances in electrocatalysts for oxygen evolution reaction of water electrolysis-from metal oxides to carbon nanotubes. *Progress in natural science: materials international*, *25*(6), 545-553.

Ćirić-Marjanović, G. (2013). Recent advances in polyaniline research: Polymerization mechanisms, structural aspects, properties and applications. *Synthetic Metals*, *177*, 1-47.

Daniel, D. K., Mankidy, B. D., Ambarish, K., & Manogari, R. (2009). Construction and operation of a microbial fuel cell for electricity generation from wastewater. *International journal of hydrogen energy*, *34*(17), 7555-7560.

Das, I., Ghangrekar, M., Satyakam, R., Srivastava, P., Khan, S., & Pandey, H. (2020). On-site sanitary wastewater treatment system using 720-L stacked microbial fuel cell: case study. *Journal of Hazardous, Toxic, and Radioactive Waste*, *24*(3), 04020025.

Dbira, S., Bensalah, N., Ahmad, M. I., & Bedoui, A. (2019). Electrochemical oxidation/disinfection of urine wastewaters with different anode materials. *Materials*, *12*(8), 1254.

De Yoreo, J. (2020). A perspective on multistep pathways of nucleation. In *Crystallization via Nonclassical Pathways Volume 1: Nucleation, Assembly, Observation & Application* (pp. 1-17). ACS Publications.

Denis, M., Jeanneau, L., Pierson-Wickman, A.-C., Humbert, G., Petitjean, P., Jaffrézic, A., & Gruau, G. (2017). A comparative study on the pore-size and filter type effect on the molecular composition of soil and stream dissolved organic matter. *Organic geochemistry*, *110*, 36-44.

Doane, T. A., Silva, L. C., & Horwath, W. R. (2019). Exposure to light elicits a spectrum of chemical changes in soil. *Journal of Geophysical Research: Earth Surface*, *124*(8), 2288-2310.

Dumas, C., Mollica, A., Féron, D., Basséguy, R., Etcheverry, L., & Bergel, A. (2007). Marine microbial fuel cell: use of stainless steel electrodes as anode and cathode materials. *Electrochimica Acta*, *53*(2), 468-473.

Ebba, M., Asaithambi, P., & Alemayehu, E. (2022). Development of electrocoagulation process for wastewater treatment: optimization by response surface methodology. *Heliyon*, *8*(5).

Elmas, S., Macdonald, T. J., Skinner, W., Andersson, M., & Nann, T. (2019). Copper metallopolymer catalyst for the electrocatalytic hydrogen evolution reaction (HER). *Polymers*, *11*(1), 110.

Emeji, I. C., Ama, O. M., Aigbe, U. O., Khoele, K., Osifo, P. O., & Ray, S. S. (2020). Electrochemical cells. *Nanostructured Metal-Oxide Electrode Materials for Water Purification: Fabrication, Electrochemistry and Applications*, 65-84.

Ferroni, L., Brestič, M., Živčak, M., Cantelli, R., & Pancaldi, S. (2021). Increased photosynthesis from a deep-shade to high-light regime occurs by enhanced CO_2 diffusion into the leaf of Selaginella martensii. *Plant Physiology and Biochemistry*, *160*, 143-154.

Findlay, S. E. G. (2021). Organic matter decomposition. In *Fundamentals of ecosystem science* (2nd ed., pp. 81–102). https://doi.org/10.1016/B978-0-12-812762-9.00004-6

Firdous, S., Jin, W., Shahid, N., Bhatti, Z., Iqbal, A., Abbasi, U., Mahmood, Q., & Ali, A. (2018). The performance of microbial fuel cells treating vegetable oil industrial wastewater. *Environmental technology & innovation*, *10*, 143-151.

Ganiyu, S. O., & El-Din, M. G. (2020). Insight into in-situ radical and non-radical oxidative degradation of organic compounds in complex real matrix during electrooxidation with boron doped diamond electrode: A case study of oil sands process water treatment. *Applied Catalysis B: Environmental*, *279*, 119366.

Ganiyu, S. O., Martínez-Huitle, C. A., & Oturan, M. A. (2018). Electrochemical advanced oxidation processes for wastewater treatment: Advances in formation and detection of reactive species and mechanistic pathways. *Applied Catalysis B: Environmental, 235,* 103–129. https://doi.org/10.1016/j.apcatb.2018.04.010

Ganiyu, S. O., Martínez-Huitle, C. A., & Rodrigo, M. A. (2020). Electrochemical advanced oxidation processes: A review on the mechanistic, kinetic and performance aspects for the degradation of organic pollutants. *Electrochimica Acta, 338,* 135809. https://doi.org/10.1016/j.electacta.2020.135809

García-Espinoza, J. D., Robles, I., Durán-Moreno, A., & Godínez, L. A. (2021). Photo-assisted electrochemical advanced oxidation processes for the disinfection of aqueous solutions: A review. *Chemosphere*, *274*, 129957.

Garcia-Segura, S., Lanzarini-Lopes, M., Hristovski, K., & Westerhoff, P. (2021). Electrocatalytic and photocatalytic nanomaterials for water treatment: Mechanisms, efficiency, and cost considerations. *Chemical Engineering Journal, 404,* 126583. https://doi.org/10.1016/j.cej.2020.126583

Gavali, D. S., & Thapa, R. (2021). Synergetic effect of localized and delocalized π electron on Li storage properties of Si/C heterostructures. *Carbon*, *171*, 257-264.

Gebel, G. (2000). Structural evolution of water swollen perfluorosulfonated ionomers from dry membrane to solution. *polymer*, *41*(15), 5829-5838.

Gemünde, A., Lai, B., Pause, L., Krömer, J., & Holtmann, D. (2022). Redox mediators in microbial electrochemical systems. *ChemElectroChem*, *9*(13), e202200216.

Ghasemi, M., Khataee, A., Gholami, P., Soltani, R. D. C., Hassani, A., & Orooji, Y. (2020). In-situ electro-generation and activation of hydrogen peroxide using a CuFeNLDH-CNTs modified graphite cathode for degradation of cefazolin. *Journal of environmental management*, *267*, 110629.

Ghassemi, Z., & Slaughter, G. (2017). Biological fuel cells and membranes. *Membranes*, *7*(1), 3-26.

Goral, M., Swadzba, L., Moskal, G., Hetmanczyk, M., & Tetsui, T. (2009). Si-modified aluminide coatings deposited on Ti46Al7Nb alloy by slurry method. *Intermetallics*, *17*(11), 965-967.

Hansen, A. M., Kraus, T. E., Pellerin, B. A., Fleck, J. A., Downing, B. D., & Bergamaschi, B. A. (2016). Optical properties of dissolved organic matter (DOM): Effects of biological and photolytic degradation. *Limnology and oceanography*, *61*(3), 1015-1032.

Henze, M., & Ledin, A. (2001). Types, characteristics and quantities of classic, combined domestic wastewaters. In *Decentralised sanitation and reuse: Concepts, systems and implementation* (pp. 59-72). IWA Publishing.

Ho, Y., McKay, G., Wase, D., & Forster, C. (2000). Study of the sorption of divalent metal ions on to peat. *Adsorption science & technology*, *18*(7), 639-650.

Huang, L., Zaman, S., Tian, X., Wang, Z., Fang, W., & Xia, B. Y. (2021). Advanced platinum-based oxygen reduction electrocatalysts for fuel cells. *Accounts of chemical research*, *54*(2), 311-322.

Huang, H., Yao, J., Li, L., Zhu, F., Liu, Z., Zeng, X., Yu, X., & Huang, Z. (2016). Reinforced polyaniline/polyvinyl alcohol conducting hydrogel from a freezing–thawing method as self-supported electrode for supercapacitors. *Journal of Materials Science*, *51*, 8728-8736.

Hunsom, M., Pruksathorn, K., Damronglerd, S., Vergnes, H., & Duverneuil, P. (2005). Electrochemical treatment of heavy metals (Cu2+, Cr6+, Ni2+) from industrial effluent and modeling of copper reduction. *Water Research*, *39*(4), 610-616.

Ibanez, J. G., Rincón, M. E., Gutierrez-Granados, S., Chahma, M. h., Jaramillo-Quintero, O. A., & Frontana-Uribe, B. A. (2018). Conducting polymers in the fields of energy, environmental remediation, and chemical–chiral sensors. *Chemical reviews*, *118*(9), 4731-4816.

Ike, I. A., Lee, Y., & Hur, J. (2019). Impacts of advanced oxidation processes on disinfection byproducts from dissolved organic matter upon post-chlor (am) ination: A critical review. *Chemical Engineering Journal*, *375*, 121929.

Islam, N., Wang, H., Maqbool, F., & Ferro, V. (2019). In vitro enzymatic digestibility of glutaraldehyde-crosslinked chitosan nanoparticles in lysozyme solution and their applicability in pulmonary drug delivery. *Molecules*, *24*(7), 1271.

Jamadade, V., Dhawale, D., & Lokhande, C. (2010). Studies on electrosynthesized leucoemeraldine, emeraldine and pernigraniline forms of polyaniline films and their supercapacitive behavior. *Synthetic Metals*, *160*(9-10), 955-960.

Jiao, R., Xu, H., Xu, W., Yang, X., & Wang, D. (2015). Influence of coagulation mechanisms on the residual aluminum–The roles of coagulant species and MW of organic matter. *Journal of Hazardous Materials*, *290*, 16-25.

Kadari, M., Belarbi, E. H., Moumene, T., Bresson, S., Haddad, B., Abbas, O., & Khelifa, B. (2017). Comparative study between 1-Propyl-3-methylimidazolium bromide and trimethylene bis-methylimidazolium bromide ionic liquids by FTIR/ATR and FT-RAMAN spectroscopies. *Journal of Molecular Structure*, *1143*, 91-99.

Khan, H., Yerramilli, A. S., D'Oliveira, A., Alford, T. L., Boffito, D. C., & Patience, G. S. (2020). Experimental methods in chemical engineering: X-ray diffraction spectroscopy—XRD. *The Canadian journal of chemical engineering*, *98*(6), 1255-1266.

Khotseng, L. (2018). Oxygen reduction reaction. *Electrocatalysts for fuel cells and hydrogen evolution-Theory to design*, 27.

Kongkanand, A., Yarlagadda, V., Gu, W., & Arisetty, S. (2023). Platinum surface oxide and oxygen reduction reaction kinetics during transient fuel cell operation. *Journal of The Electrochemical Society*, *170*(9), 094506.

Koroglu, E. O., Yoruklu, H. C., Demir, A., & Ozkaya, B. (2019). Scale-up and commercialization issues of the MFCs: challenges and implications. In *Microbial electrochemical technology* (pp. 565-583). Elsevier.

Krupińska, I. (2020). Aluminium drinking water treatment residuals and their toxic impact on human health. *Molecules*, *25*(3), 641.

Ksibi, M. (2006). Chemical oxidation with hydrogen peroxide for domestic wastewater treatment. *Chemical Engineering Journal*, *119*(2-3), 161-165.

Kumar, S., Singh, S., & Srivastava, V. C. (2015). Electro-oxidation of nitrophenol by ruthenium oxide coated titanium electrode: parametric, kinetic and mechanistic study. *Chemical Engineering Journal*, *263*, 135-143.

Lee, J. S., You, K. H., & Park, C. B. (2012). Highly photoactive, low bandgap TiO2 nanoparticles wrapped by graphene. *Advanced materials*, *24*(8), 1084-1088.

Lei, X., Pan, J., & Devlin, A. T. (2019). Characteristics of absorption spectra of chromophoric dissolved organic matter in the pearl river estuary in spring. *Remote Sensing*, *11*(13), 1533.

Leong, D., Teo, K., Rangarajan, S., Lopez-Jaramillo, P., Avezum Jr, A., & Orlandini, A. (2018). World Population Prospects 2019. Department of Economic and Social Affairs Population Dynamics. New York (NY): United Nations; 2019 (https://population. un. org/wpp/Download/, accessed 20 September 2020). The decade of healthy ageing. Geneva: World Health Organization. *World*, *73*(7), 362k2469.

Liu, H., Ramnarayanan, R., & Logan, B. E. (2020). Production of electricity during wastewater treatment using a single chamber microbial fuel cell. *Environmental Science & Technology, 38*(7), 2281–2285. https://doi.org/10.1021/es034923g

Li, N., Shi, L., Wang, X., Guo, F., & Yan, C. (2011). Experimental Study of Closed System in the Chlorine Dioxide-Iodide-Sulfuric Acid Reaction by UV-Vis Spectrophotometric Method. *International journal of analytical chemistry*, *2011*(1), 130102.

Li, P., & Hur, J. (2017). Utilization of UV-Vis spectroscopy and related data analyses for dissolved organic matter (DOM) studies: A review. *Critical Reviews in Environmental Science and Technology*, *47*(3), 131-154.

Liang, G. (2022). Iron uptake, signaling, and sensing in plants. *Plant Communications*, 3(5).

Logan, B. E., & Rabaey, K. (2019). Conversion of wastes into bioelectricity and chemicals by using microbial electrochemical technologies. *Science, 337*(6095), 686–690. https://doi.org/10.1126/science.1217412

Logan, B. E., Hamelers, B., Rozendal, R., Schröder, U., Keller, J., Freguia, S., Aelterman, P., Verstraete, W., & Rabaey, K. (2006). Microbial fuel cells: methodology and technology. *Environmental Science & Technology*, *40*(17), 5181-5192.

Louis, M. N., & Gabriel, B. O. (2014). Colour of starch-iodine complex as index of retrogradability of starch pastes. *African Journal of Pure and Applied Chemistry*, *8*(5), 89-93.

Lu, Y., Alvarez, A., Kao, C.-H., Bow, J.-S., Chen, S.-Y., & Chen, I.-W. (2019). An electronic silicon-based memristor with a high switching uniformity. *Nature Electronics*, *2*(2), 66-74.

Mansoorian, H. J., Mahvi, A. H., Jafari, A. J., & Khanjani, N. (2016). Evaluation of dairy industry wastewater treatment and simultaneous bioelectricity generation in a catalyst-

less and mediator-less membrane microbial fuel cell. *Journal of Saudi Chemical Society*, *20*(1), 88-100.

Martínez-Huitle, C. A., & Andrade, L. S. (2011). Electrocatalysis in wastewater treatment: recent mechanism advances. *Quimica Nova*, *34*, 850-858.

Martínez-Huitle, C. A., & Ferro, S. (2016). Electrochemical oxidation of organic pollutants for wastewater treatment: Direct and indirect processes. *Chemical Society Reviews, 35*(12), 1324–1340. https://doi.org/10.1039/B517632H

Mathew, M. (2000). *Quality attributes of selected leafy vegetables* (Doctoral dissertation, Department of Home Science, College of Horticulture, Vellanikkara).

Matis, K., & Peleka, E. (2010). Alternative flotation techniques for wastewater treatment: focus on electroflotation. *Separation Science and Technology*, *45*(16), 2465-2474.

Mayerhöfer, T. G., Pahlow, S., & Popp, J. (2020). The Bouguer-Beer-Lambert law: Shining light on the obscure. *Chemical physics and Physical Chemistry*, *21*(18), 2029-2046.

de Mello, V. M., de Lima Santos, D. D., Freitas, R. C. S., Yokoyama, L., & Cammarota, M. C. (2018). Energy generation in the treatment of effluent from washing of municipal solid waste collection trucks. *Sustainable Energy Technologies and Assessments, 30*, 105–113. https://doi.org/10.1016/j.seta.2018.09.009

Miklos, D. B., Remy, C., Jekel, M., Linden, K. G., Drewes, J. E., & Hübner, U. (2018). Evaluation of advanced oxidation processes for water and wastewater treatment–A critical review. *Water Research*, *139*, 118-131.

Molapo, K. M., Ndangili, P. M., Ajayi, R. F., Mbambisa, G., Mailu, S. M., Njomo, N., Masikini, M., & Iwuoha, P. B. I. (2012). Electronics of conjugated polymers (I): polyaniline. *International Journal of Electrochemical Science, 7*(12), 11859-11875.

Moradi, V., Jun, M. B., Blackburn, A., & Herring, R. A. (2018). Significant improvement in visible light photocatalytic activity of Fe doped TiO2 using an acid treatment process. *Applied Surface Science*, *427*, 791-799.

Morris, A. L., & Mohiuddin, S. S. (2020). Biochemistry, nutrients.

Moulay, S. (2013). Molecular iodine/polymer complexes. *Journal of Polymer Engineering*, *33*(5), 389-443.

Mukamel, S. (2000). Multidimensional femtosecond correlation spectroscopies of electronic and vibrational excitations. *Annual Review of Physical Chemistry*, *51*(1), 691-729.

Mwangi, I., Kiriro, G., Swaleh, S., Wanjau, R., Mbugua, P., & Ngila, J. C. (2019). Remediation of degraded soils with hydrogels from domestic animal wastes. *International Journal of Recycling of Organic Waste in Agriculture*, *8*, 159-170.

Mwangi, I. W., Ngila, J. C., Ndungu, P., Msagati, T. A., & Kamau, J. N. (2013). Immobilized Fe (III)-doped titanium dioxide for photodegradation of dissolved organic compounds in water. *Environmental Science and Pollution Research*, *20*, 6028-6038.

Naidoo, S., & Olaniran, A. O. (2014). Treated wastewater effluent as a source of microbial pollution of surface water resources. *International Journal of Environmental Research and Public Health*, *11*(1), 249-270.

Natesh, H. N., Abbey, L., & Asiedu, S. K. (2017). An overview of nutritional and antinutritional factors in green leafy vegetables. *Horticulture International Journal*, *1*(2), 58-65.

Nawaz, H., Shi, J., Mittal, G. S., & Kakuda, Y. (2006). Extraction of polyphenols from grape seeds and concentration by ultrafiltration. *Separation and Purification Technology*, *48*(2), 176-181.

Outten, F. W., & Theil, E. C. (2009). Iron-based redox switches in biology. *Antioxidants & Redox signaling*, *11*(5), 1029-1046.

Özyurt, B., & Camcıoğlu, Ş. (2018). Applications of combined electrocoagulation and electrooxidation treatment to industrial wastewaters. *Wastewater and Water Quality*, *56*(1), 71-89.

Panizza, M., & Cerisola, G. (2008). Electrochemical degradation of methyl red using BDD and PbO2 anodes. *Industrial & Engineering Chemistry Research*, *47*(18), 6816-6820.

Pathiraja, G. C., Jayathilaka, P. B., Weerakkody, C., Karunarathne, P., & Nanayakkara, N. (2014). Comparison study of dimensionally stable anodes for degradation of chlorpyrifos in water. *Current Science*, 219-226.

Paul, T. C. (2018). Structural, electrical and optical characterization of fe and zn doped tio2 thin films prepared by spray pyrolysis technique.*and public health*, *11*(1), 249-270.

Pei, D.-N., Liu, C., Zhang, A.-Y., Pan, X.-Q., & Yu, H.-Q. (2020). In situ organic Fenton-like catalysis triggered by anodic polymeric intermediates for electrochemical water purification. *Proceedings of the National Academy of Sciences*, *117*(49), 30966-30972.

Peter, S. C. (2018). Reduction of CO_2 to chemicals and fuels: a solution to global warming and energy crisis. *ACS Energy Letters*, *3*(7), 1557-1561.

Pipi, A. R., Aquino Neto, S., & Andrade, A. R. D. (2013). Electrochemical degradation of diuron in chloride medium using DSA® based anodes. *Journal of the Brazilian Chemical Society*, *24*, 1259-1266.

Platt, C. (2009). *Make: Electronics: Learning Through Discovery*. " O'Reilly Media, Inc.".

Prakasham, R. S., & Kumar, B. S. (2019). Bacterial metabolism–coupled energetics. In S. Venkata Mohan, S. Varjani, & A. Pandey (Eds.), *Microbial electrochemical technology* (pp. 227–260). Elsevier. https://doi.org/10.1016/B978-0-444-64052-9.00009-1

Porter, I. J., Cushing, S. K., Carneiro, L. M., Lee, A., Ondry, J. C., Dahl, J. C., Chang, H.-T., Alivisatos, A. P., & Leone, S. R. (2018). Photoexcited small polaron formation in goethite (α-FeOOH) nanorods probed by transient extreme ultraviolet spectroscopy. *The journal of physical chemistry letters*, *9*(14), 4120-4124.

Rahimnejad, M. (2023). MFC designing and performance. *Biological Fuel Cells* (pp. 147-175). Elsevier.

Rasalingam, S., Peng, R., & Koodali, R. T. (2014). Removal of hazardous pollutants from wastewaters: applications of TiO 2-SiO 2 mixed oxide materials. *Journal of Nanomaterials*, *2014*, 10-10.

Redel, E., Röhr, C., & Janiak, C. (2009). An inorganic starch–iodine model: the inorganic–organic hybrid compound {(C 4 H 12 N 2) 2 [Cu II 4](I 2)} n. *Chemical communications*(16), 2103-2105.

Reguera, G. (2018). Microbial nanowires and electroactive biofilms. *FEMS Microbiology Ecology, 94*(7), fiy086. https://doi.org/10.1093/femsec/fiy086

Reimers, C., Girguis, P., Stecher, H., Tender, L., Ryckelynck, N., & Whaling, P. (2006). Microbial fuel cell energy from an ocean cold seep. *Geobiology*, *4*(2), 123-136.

Richter, H., McCarthy, K., Nevin, K. P., Johnson, J. P., Rotello, V. M., & Lovley, D. R. (2008). Electricity generation by Geobacter sulfurreducens attached to gold electrodes. *Langmuir*, *24*(8), 4376-4379.

Roy, H., Rahman, T. U., Tasnim, N., Arju, J., Rafid, M. M., Islam, M. R., Pervez, M. N., Cai, Y., Naddeo, V., & Islam, M. S. (2023). Microbial Fuel Cell Construction Features and Application for Sustainable Wastewater Treatment. *Membranes*, *13*(5), 490.

Ruzgys, P., Novickij, V., Novickij, J., & Šatkauskas, S. (2019). Influence of the electrode material on ROS generation and electroporation efficiency in low and high frequency nanosecond pulse range. *Bioelectrochemistry*, *127*, 87-93.

Ryan, D. R., Maher, E. K., Heffron, J., Mayer, B. K., & McNamara, P. J. (2021). Electrocoagulation-electrooxidation for mitigating trace organic compounds in model drinking water sources. *Chemosphere*, *273*, 129377.

Saif, T., Lin, Q., Butcher, A. R., Bijeljic, B., & Blunt, M. J. (2017). Multi-scale multi-dimensional microstructure imaging of oil shale pyrolysis using X-ray micro-tomography, automated ultra-high resolution SEM, MAPS Mineralogy and FIB-SEM. *Applied energy*, *202*, 628-647.

Samer, M. (2015). Biological and chemical wastewater treatment processes. *Wastewater treatment engineering*, *150*, 212.

Sapurina, I., Tenkovtsev, A. V., & Stejskal, J. (2015). Conjugated polyaniline as a result of the benzidine rearrangement. *Polymer International*, *64*(4), 453-465.

Sarkar, A., & Khan, G. G. (2019). The formation and detection techniques of oxygen vacancies in titanium oxide-based nanostructures. *Nanoscale*, *11*(8), 3414-3444.

Sathe, S., Bhowmick, G., Dubey, B., & Ghangrekar, M. (2020). Surfactant removal from wastewater using photo-cathode microbial fuel cell and laterite-based hybrid treatment system. *Bioprocess and biosystems engineering*, *43*, 2075-2084.

Sen, T., Mishra, S., & Shimpi, N. G. (2016). Synthesis and sensing applications of polyaniline nanocomposites: a review. *RSC advances*, *6*(48), 42196-42222.

Sequeira, C., & Santos, D. (2009). Electrochemical routes for industrial synthesis. *Journal of the Brazilian Chemical Society*, *20*, 387-406.

Shao, Y., El-Kady, M. F., Sun, J., Li, Y., Zhang, Q., Zhu, M., Wang, H., Dunn, B., & Kaner, R. B. (2018). Design and mechanisms of asymmetric supercapacitors. *Chemical reviews*, *118*(18), 9233-9280.

Shestakova, M., & Sillanpää, M. (2017). Electrode materials used for electrochemical oxidation of organic compounds in wastewater. *Reviews in Environmental Science and Bio/Technology*, *16*(2), 223-238.

Singh, D., Pratap, D., Baranwal, Y., Kumar, B., & Chaudhary, R. (2010). Microbial fuel cells: A green technology for power generation. *Annals of biological research*, *1*(3), 128-138.

Subba Rao, A. N., & Venkatarangaiah, V. T. (2014). Metal oxide-coated anodes in wastewater treatment. *Environmental Science and Pollution Research*, *21*, 3197-3217.

Sudarsan, J., Prasanna, K., Renganathan, K., & Beigh, M. A. B. Role of Microbial Fuel Cell (Mfc) In Wastewater Treatment & Energy Prouction–A Trial Study.

Tabassum, N., Islam, N., & Ahmed, S. (2021). Progress in microbial fuel cells for sustainable management of industrial effluents. *Process Biochemistry*, *106*, 20-41.

Tan, R., Qin, Y., Liu, M., Wang, H., Li, J., Luo, Z., & Zhu, C. (2023). Nickel single-atom catalyst-mediated efficient redox cycle enables self-checking photoelectrochemical biosensing with dual photocurrent readouts. *ACS sensors*, *8*(1), 263-269.

Tao, H. C., Liang, M., Li, W., Zhang, L. J., Ni, J. R., & Wu, W. M. (2011). Removal of copper from aqueous solution by electrodeposition in cathode chamber of microbial fuel cell. *Journal of hazardous materials*, *189*(1-2), 186-192.

Toh, R. J., Peng, W. K., Han, J., & Pumera, M. (2014). Direct in vivo electrochemical detection of haemoglobin in red blood cells. *Scientific reports*, *4*(1), 6209.

Utomo, S. B., Winarto, Widodo, A. S., & Wardana, I. N. G. (2019). The Role of Mineral Sea Water Bonding Process with Graphite-Aluminum Electrodes as Electric Generator. *The Scientific World Journal*, *2019*(1), 7028316.

Vishwanathan, A. (2021). Microbial fuel cells: a comprehensive review for beginners. *3 Biotechnology*, *11*(5), 248.

Wang, C.-y., Böttcher, C., Bahnemann, D. W., & Dohrmann, J. K. (2003). A comparative study of nanometer sized Fe (III)-doped TiO 2 photocatalysts: synthesis, characterization and activity. *Journal of Materials Chemistry*, *13*(9), 2322-2329.

Wang, W., Chen, M., Wang, D., Yan, M., & Liu, Z. (2021). Different activation methods in sulfate radical-based oxidation for organic pollutants degradation: Catalytic mechanism and toxicity assessment of degradation intermediates. *Science of The Total Environment*, *772*, 145522.

Wang, W., Varghese, O. K., Paulose, M., Grimes, C. A., Wang, Q., & Dickey, E. C. (2004). A study on the growth and structure of titania nanotubes. *Journal of materials research*, *19*(2), 417-422.

Ward, C. P., & Cory, R. M. (2016). Complete and partial photo-oxidation of dissolved organic matter draining permafrost soils. *Environmental Science & Technology*, *50*(7), 3545-3553.

Weng, B., Yang, M. Q., Zhang, N., & Xu, Y. J. (2014). Toward the enhanced photoactivity and photostability of ZnO nanospheres via intimate surface coating with reduced graphene oxide. *Journal of Materials Chemistry A*, *2*(24), 9380-9389.

Woo, M., Maier, L., Tischer, S., Deutschmann, O., & Wörner, M. (2020). A qualitative numerical study on catalytic hydrogenation of nitrobenzene in gas-liquid taylor flow with detailed reaction mechanism. *Fluids*, *5*(4), 234.

Woo, Y. C., Chen, Y., Tijing, L. D., & Shon, H. K. (2020). Recent progress in electrochemical advanced oxidation processes for wastewater treatment. *Journal of Environmental Chemical Engineering, 8*(5), 104195. https://doi.org/10.1016/j.jece.2020.104195

Xu, X., Hou, Q., Xue, Y., Jian, Y., & Wang, L. (2018). Pollution characteristics and fate of microfibers in the wastewater from textile dyeing wastewater treatment plant. *Water Science and Technology*, *78*(10), 2046-2054.

Yadav, P., Nigel-Etinger, I., Kumar, A., Mizrahi, A., Mahammed, A., Fridman, N., Lipstman, S., Goldberg, I., & Gross, Z. (2021). Hydrogen evolution catalysis by terminal molybdenum-oxo complexes. iScience, 2021, 24 (8), 102924. In.

Yang, X., López-Grimau, V., Vilaseca, M., & Crespi, M. (2020). Treatment of textile wastewater by CAS, MBR, and MBBR: a comparative study from technical, economic, and environmental perspectives. *Water*, *12*(5), 1306.

Yi, H., Nevin, K. P., Kim, B.-C., Franks, A. E., Klimes, A., Tender, L. M., & Lovley, D. R. (2009). Selection of a variant of Geobacter sulfurreducens with enhanced capacity for current production in microbial fuel cells. *Biosensors and Bioelectronics*, *24*(12), 3498-3503.

Zedek, R., Djedjiga, H., Megherbi, M., Belkaid, M. S., & Ntsoenzok, E. (2021). Effects of slight Fe (III)-doping on structural and optical properties of TiO2 nanoparticles. *Journal of Sol-Gel Science and Technology*, *100*(1), 44-54.

Zeghioud, H., Lamouri, S., Safidine, Z., & Belbachir, M. (2015). Chemical synthesis and characterization of highly soluble conducting polyaniline in mixtures of common solvents. *Journal of the Serbian Chemical Society*, *80*(7), 917–931-917–931.

Zhao, L.-l., & Song, T.-s. (2014). Simultaneous carbon and nitrogen removal using a litre-scale upflow microbial fuel cell. *Water Science and Technology*, *69*(2), 293-297.

Zheng, C., Zhao, L., Zhou, X., Fu, Z., & Li, A. (2013). Treatment technologies for organic wastewater. *Water treatment*, *11*, 250-286.

APPENDICES

Appendix A: Raw Degradation Data for Green Leafy Vegetable Wastewater

Table 1: Voltage values for the degradation of starch

Time (min	Potential (V)
0	1.11
20	1.2
30	1.24
35	1.25
40	1.25
50	1.23
60	1.23
70	1.22
80	1.21

Table 2: Absorbance values of degradation of starch against time,

Time (Minutes)	Absorbance (nm)
0	2.3416
30	1.7138
60	1.1845
90	0.5859
120	0.4764
150	0.3845
180	0.2716

Table 3: Kinetic data fitted for first order expression

Time (minute)	Absorbance(nm)
0	2.3416
30	1.7138
60	1.1845
90	0.5859
120	0.4764
150	0.3845
180	0.2716

Table 4: Kinetic data fitted for second order expression

Time (Minutes)	Reciprocal Abs (1/nm)
0	0.427
30	0.5834
60	0.844
90	1.7068
120	2.099
150	2.6
180	3.681

Table 5: The variation of potential difference of the electrochemical with time

Time (Minutes)	Voltage (mV)
0	0
30	97.6
60	105
90	108.2
120	110.6
150	111.4
155	104.1
160	100.2
170	97.3
175	97
180	93.3
185	90.1
190	87.9
200	84

Table 6: The results of UV-Vis absorbance data plotted against time using dimensionally stable anode

Time (minutes)	Absorbance (nm)
0	2.4
30	1.6
55	1.2
80	0.68
120	0.544
150	0.47
175	0.4
200	0.31

Table 7: UV-Vis absorbance data plotted against time for dimensionally stable anode

Time (minutes)	Absorbance(nm)
0	2.4
1440	1.2
2880	0.4
4320	0.061
5760	0.005

Table 8: First order degradation kinetics data

Time (minutes)	ln Abs
0	0.875469
30	0.470004
60	0.182322
90	-0.38566
120	-0.60881
150	-0.75502
180	-0.91629
210	-1.17118

Table 9: Second order degradation kinetics data

Time(minutes)	1/Abs (nm^{-1})
0	2.4
30	1.6
55	1.2
80	0.68
120	0.544
150	0.47
175	0.4
200	0.31

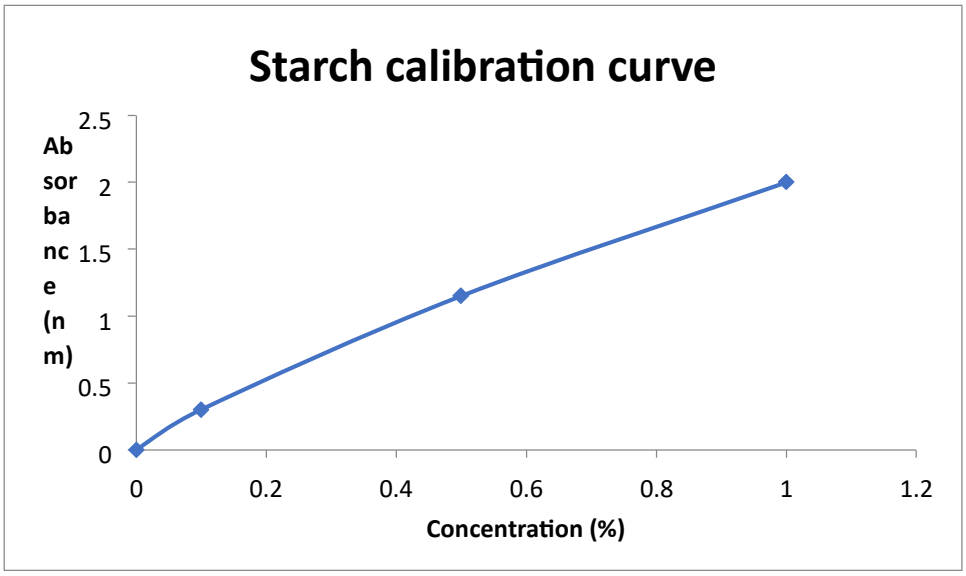

Figure 1: The starch calibration curve

Table 10: Data for starch calibration curve

Concentration (%)	Absorbance (nm)
1	2
0.5	1.15
0.1	0.3
0	0

Appendix B: Abstracts of the published articles

Heliyon 7 (2021) e06671

Contents lists available at ScienceDirect

Heliyon

journal homepage: www.cell.com/heliyon

Research article

Iron (III) doped titanium dioxide coated dimensionally stable graphite anode electrode for electro-chemical treatment of domestic wastewater

I.W. Mwangi [a,*], E.M. Kinyua [a], R. Nthumbi [a], R.N. Wanjau [a], S. Swaleh [a], J.C. Ngila [b]

[a] Department of Chemistry, Kenyatta University, P.O. Box 43844-00100, Nairobi, Kenya
[b] Department of Chemical Technology, University of Johannesburg, Doornfontein Campus, P.O Box 17011, Doornfontein 2028, Johannesburg, South Africa

ARTICLE INFO

Keywords:
Electrochemical cell
Proton exchange membrane
Oxidation
Pollution
Domestic
Wastewater

ABSTRACT

Availability of clean water is of concern due to pollution and diminishing supply pollution. However, purification is possible depending on the incorporated contaminants. Domestic wastewater contains dissolved organic matter and its remediation can be done by oxidation. The best oxidation can be achieved by electron transfer the same way metabolic processes occur. This study exploited the use of a film of iron (III) doped titanium dioxide applied on an electrode which was found to be effective. Natural light conditions generated electrons that migrated through the electrode leaving behind holes which oxidized the contaminants as the excess electrons were discharged at the cathode after passing through the casted proton exchange membrane (PEM) separating the two half cells of the prepared reactor. This electrochemical method has the advantage in that the organic pollutants are oxidized to carbon dioxide with no secondary pollutants and the inorganic pollutants into insoluble matter. The assembled cell was applied to purify both synthetic and real water samples of green leafy vegetable solution from the kitchen by clarification. The clarification process was monitored by UV-Vis using distilled water as a reference to compare the light that transmitted through a sample. It was observed that the electro-oxidation process took place showing a high potential 105 mV within the first 150 min followed by degradation at a high rate. The oxidation of the organic matter was confirmed by UV-Vis analysis as well as by cyclic voltametric analysis of iron released into the solution of the synthetic samples. The electro chemical treatment of the water was then applied to purify real water samples made from a sample of 4.5 g minced of green vegetables dispersed in one liter of water (4.5 g/l). The green leafy coloured solution was clarified after 154 h of continuous oxidation. The degradation process was confirmed to be independent of intermediates or other species present in solution as it was of first order reaction kinetics. The electrochemical oxidation of organic matter in water using iron (III) doped titanium dioxide coated graphite electrode has potential application on the purification of water.

Journal of the Iranian Chemical Society
https://doi.org/10.1007/s13738-020-02043-5

ORIGINAL PAPER

Remediation of domestic wastewater by electrochemical oxidation of dissolved organic species

Isaac Mwangi[1] · Esther Kinyua[1] · Ruth Wanjau[1] · Sauda Swaleh[1] · Jane Catherine Ngila[2]

Received: 4 September 2019 / Accepted: 17 August 2020

Abstract
This study reports on the treatment of wastewater containing dissolved organic matter (DOM). DOM introduces complexing agents, promotes bacterial growth, and affects the color plus taste of water negatively. The normal practice for treatment such pollutants is the use of introduction of oxidizing agents in the water. However, this introduces secondary pollutants to the treated water, and to overcome the challenge, this study has developed an electrochemical method for treating wastewater with no secondary pollutants. A two-chamber electrochemical cell separated by a proton exchange membrane (PEM) was constructed with inert electrodes. The PEM was made from a conducting polymer inert in aqueous media. The anode water was bubbled with air for reduction of oxygen and therefore formation of strong oxidizing agent for the degradation of DOM. The degradation was monitored using Ultraviolet–visible (UV–VIS) spectroscopy as the potential difference across the cell was monitored. There was a significant reduction in the color and the decay followed first-order kinetics, for unimolecular degradation with a constant of 0.0148 min^{-1}. A high potential of 1.25 V was registered within the first 40 min confirming that the degradation was spontaneous making the water safe for consumption. The degradation was confirmed by voltametric method where the concentration of iron within the vegetative matter was observed to increase at a potential of − 0.18 V with time due to the release of the labile metal ions. This shows that the constructed cell has a potential application in the remediation of domestic wastewater at a point of use.

Keywords Electrochemical cell · Proton exchange membrane · Oxidation · Pollution · Wastewater